International
Progress Report

IPR-99-07

Äspö Hard Rock Laboratory

TRUE Block Scale Project

Scientific and technical status

Position report prepared for the 2nd TRUE Block Scale review meeting

Stockholm, Nov 17, 1998

Anders Winberg

Conterra AB, Gothenburg, Sweden

December 1998

Svensk Kärnbränslehantering AB
Swedish Nuclear Fuel
and Waste Management Co
Box 5864
SE-102 40 Stockholm Sweden
Tel 08-459 84 00
+46 8 459 84 00
Fax 08-661 57 19
+46 8 661 57 19

Äspö Hard Rock Laboratory

Äspö Hard Rock Laboratory

TRUE Block Scale Project

Scientific and technical status

Position report prepared for the 2nd TRUE Block Scale review meeting

Stockholm, Nov 17, 1998

Anders Winberg (Ed.)

Conterra AB, Gothenburg, Sweden

December 1998

Keywords: block scale, fracture network, hydraulic model, structural model, tracer test

Foreword

This report presents the current understanding of the TRUE Block Scale rock volume. In addition the prospects for future transport experiments are reviewed and the original general project objectives are revisited and rephrased. Finally, the report gives and outlook on alternative strategies to meet the updated project objectives.

The author is grateful for the thorough review of the final draft of this report provided by Thomas Doe, Golder Associates. Comments on draft version of this report given by Peter Meier, ANDRA, Peter Andersson, GEOSIGMA AB, Jan Hermanson, Golder Grundteknik AB and Les Knight, Nirex are also gratefully acknowledged.

Abstract

This report presents the current understanding of the TRUE Block Scale rock volume. This includes a presentation of a developed hydraulic model, a structural model and an integrated discussion of natural groundwater flow. In addition the prospects for future transport experiments are reviewed supported by performed tracer dilution tests and cross-hole interference tests. In addition the original project objectives are revisited and rephrased. Finally, the report gives and outlook on alternative strategies to meet the updated project objectives.

Specifically it is shown that;

1) an interconnected network of deterministic conductive structures has been identified that may be observed in a number of boreholes. The structures are relatively well known geometrically and structurally. Consistency in hydraulic connectivity is proven from observation of pressure responses during drilling and from hydraulic cross-hole interference tests,

2) relatively well-defined hydraulic structures have been identified which constitute the boundaries to the outlined block,

3) the transmissivity range of the structures making up the identified network is less than $7 \cdot 10^{-7}$ m^2/s,

4) a conceptual model has been developed for natural groundwater flow in the structures supported by geometrical, structural and hydraulic field data. Additional support is provided by performed numerical modelling and independent geochemical data,

5) a number of candidate sections for establishing source and sink sections for future tracer experiments are available in the existing borehole array,

6) tracer tests can be successfully performed in the identified network of structures at a length scale in excess of 16 m over reasonable time frames, as evidenced by the results from one flow path.

Contents

1 Introduction

The TRUE Block Scale project is an international partnership funded by ANDRA, ENRESA, Nirex, POSIVA, PNC and SKB. The Block Scale project is one part of the Tracer Retention Understanding Experiments (TRUE) conducted at the Äspö Hard Rock Laboratory. The TRUE Block Scale project is divided into five basic stages;

- Scoping stage (1996-1997)
- Preliminary Characterisation stage (1997-1998)
- Detailed Characterisation stage (1998-1999)
- Tracer test stage (1999-2000)
- Evaluation stage (2000)

This report summarises the present understanding within the TRUE Block Scale Project including inferences based on the results of the Scoping Stage, the Preliminary Characterisation Stage, and Phase I of the Detailed Characterisation Stage.

In this reporting a review is given of the following:

- the site characterisation performed
- the hydraulic model
- the structural model
- the current understanding of groundwater flow
- the potential for future tracer tests
- the updated objectives of the project
- a methodology for achieving the project objectives

2 Objectives of project

The overall objectives of the Tracer Retention Understanding Experiments (TRUE) [1] are to:

- develop an understanding of radionuclide migration and retention in fractured rock.
- evaluate to what extent concepts used in models are based on realistic descriptions of a rock volume and if adequate data can be collected in site characterisation.
- evaluate the usefulness and feasibility of different approaches to model radionuclide migration and retention.
- provide *in-situ* data on radionuclide migration and retention.

The specific objectives of the TRUE Block Scale Project given in the test plan [2] are:

1. increase understanding of tracer transport in a fracture network and improve predictive capabilities,
2. assess the importance of tracer retention mechanisms (diffusion and sorption) in a fracture network,
3. assess the link between flow and transport data as a means for predicting transport phenomena,

These specific objectives are general in their definition. In the concluding chapter of this report updated specific objectives are given reflecting the present status of knowledge and the potential for future transport experiments.

It should be emphasised that the above plans anticipated that the planned transport experiments would use conductors with a transmissivity in the range $5 \cdot 10^{-8} - 5 \cdot 10^{-7}$ m^2/s over a length scale of 10 to 50 m. The results from the TRUE-1 Detailed Scale experiment [3] provided a basis for these expectations.

3 Experimental strategy

The project has adopted an iterative investigation approach whereby the information from each new borehole supports a formal updating of the conceptual model of the investigated rock volume. This process has produced an original structural model (March 1997) and two updates (October 1997, September 1998). A fourth structural model update is pending and is expected in December 1998.

The original plans specified using similarly updated numerical flow models to design experiments and position new boreholes. This has proved to be difficult to realise in that development of Discrete Feature Network (DFN) models is quite resource intensive. Consequently, the development of numerical models has been intensified towards the end of the Preliminary Characterisation stage. In this context two additional model concepts have been introduced; Stochastic Continuum (SC) and Channel Network (CN) models.

The project presently faces a decision regarding the need for additional boreholes. Specifically, is the current array of six boreholes sufficient for the project's objectives, or do these objectives require an additional hole. The justifications for such a hole would include 1) supplying necessary additional structural, geometrical, and hydraulic information, and/or 2) fulfilling a need for additional injection and pumping points.

4 Overview of site characterisation

4.1 Boreholes

The available collar positions for accessing the TRUE Block Scale rock volume are limited to the available system of tunnels in the southwest part of the Äspö Hard Rock Laboratory. The boreholes that sample the TRUE Block Scale rock volume are listed in Table 4-1. These boreholes are visualised in Figure 4-1. Three of the boreholes (KI0025F, KI0023B and KI0025F02) have been drilled using a 76-mm triple tube core barrel in order to obtain the best possible quality in the retrieved drill cores. In addition, this technique improves the retrieval of unconsolidated core material in fracture infillings, which is highly relevant to understanding retention processes.

Table 4-1 List of collar coordinates in Äspö Local System, bearing, inclination and length of relevant boreholes used in the TRUE Block Scale Project. A negative inclination implies vertically down.

Borehole	Easting (m)	Northing (m)	Elevation (masl)	Bearing (deg)	Inclination (deg)	Length (m)
KA2511A	2020.08	7211.81	-335.83	234.8	-33.4	293.0
KA2563A	2025.57	7271.54	-340.79	237.2	-42.5	363.4
KA3510A	1953.80	7260.89	-448.70	255.3	-30.2	150.1
KI0025F	1954.69	7238.15	-448.23	187.1	-20.2	193.8
KI0023B	1951.91	7241.26	-447.69	214.6	-20.7	200.7
KI0025F02	1952.80	7238.62	-448.47	200.2	-25.0	204.2
KA3573A	1893.28	7270.90	-446.07	188.3	-2.1	40.1
KA3600F	1866.01	7275.46	-445.58	248.4	-1.7	50.1

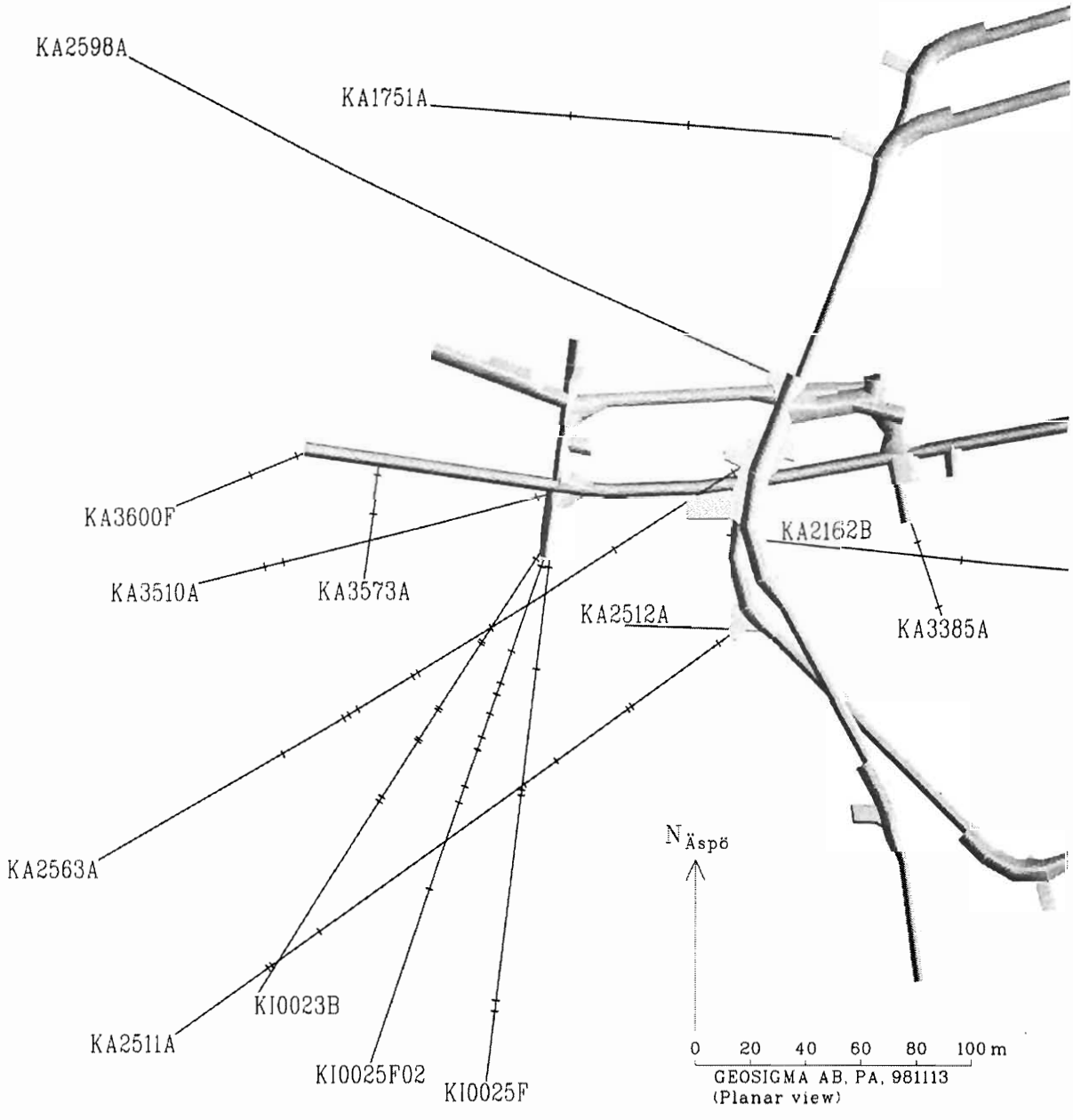

Figure 4-1 Plan view of boreholes penetrating the TRUE Block Scale volume used for pressure monitoring. The tics on the borehole projections represent packer positions as of May 1998. The packed-off sections are detailed in Appendix A.

4.2 Characterisation in single holes

During core drilling careful measurements of inflow were made between uptakes. Effectively, this procedure provides an early identification of the major conducting structures in the borehole. The identification of hydraulic structures is further enhanced by the use of the borehole imaging system (BIPS) and borehole radar employing both directional (60 MHz) and high-frequency (250 Mhz). The directional radar survey also provides information away from the borehole wall.

Three different types of flow logging techniques have been employed to identify the location of hydraulic structures -- the acoustic UCM flow meter, the double packer flow logging method and the POSIVA flow meter. The latter two methods also yield estimates of the transmissivity of the tested section in addition to identifying the locations of the flowing fractures. The POSIVA flow meter and the BIPS imaging together provide a powerful method for identifying and quantifying conductive fractures. This combination was tested for the first time in the most recent borehole KI0025F02.

The final step in the single hole hydraulic characterisation is transient flow and pressure build up tests performed in selected sections. These tests provide more reliable estimates of the transmissivity and also provide information on flow regime, flow geometry, and local hydraulic boundaries. These tests are for the most part carried out as constant pressure tests.

4.3 Cross-hole characterisation

The project used several methods of cross-hole characterisation in existing boreholes. The simplest of the methods uses pressure responses during drilling. A comparison of pressure responses in observation holes with water inflow and drilling depth in the borehole being drilled, provides an effective check on the consistency and validity of the present structural model. Likewise, it provides essential information for updating the structural model. Quantitative interpretation of pressure responses to drilling, however, is complicated by the multiple sources and short-circuiting that occurs in the open drill hole.

4.3.1 Cross-hole hydraulic tests

A series of hydraulic cross-hole interference tests have been performed between March and May 1998. The objective was to test two hypotheses regarding the nature of connections among the hydraulically dominant, NW-trending subvertical structures. The first hypothesis explained these connections using NE-trending subvertical features. The second hypothesis used a subhorizontal set of conductors to connect the NW

structures. A series of 19 cross-hole interference tests were performed using pumping durations ranging from 0.5 to 384 hours. The longer tests were carried out as constant-rate tests, and the short-time tests were carried out as constant pressure tests. In the case of the longer tests (flow period > 0.5 hr) tracer dilution tests were performed in a selection of test sections in adjacent boreholes. The dilution tests provided information on flow rates in some of the observation intervals to complement the information on transient pressure responses. In one case the pumping was prolonged to study the breakthrough of tracer in the pumped section. The cross-hole interference tests provide data for both model predictions, model calibrations and conceptual model development.

During the characterisation of the new borehole KI0025F02 a new sequencing of hydraulic tests was utilised. A number of short-duration cross-hole interference tests with the source in the new borehole preceded the flow and pressure build-up tests [4]. These tests were followed by a repetition of two of the initial interference tests, this time with simultaneous tracer dilution tests in three selected sections in the neighbouring boreholes. The preliminary results of these tests provided information for designing the multi-packer system that has been installed in the borehole. Following packer installation, the testing was reversed with pumping in one selected section in a neighbouring borehole and simultaneous injection of tracer in three sections in the new borehole.

4.3.2 Cross-hole seismic investigations

A cross-hole seismic testing campaign was performed late in 1996 between boreholes KA2511A and KA2563A. A number of seismic reflectors (N=10) were identified as a result of this study. However, due to the fact that the two boreholes make up a plane (the boreholes were not primarily drilled to facilitate cross-hole seismics) the geometrical interpretation suffered from a high degree of ambiguity.

During Dec 1997-Jan 1998, a second, three-dimensional, seismic testing campaign was carried out. In this case using the borehole KI0023B as a receiver hole. A portable seismic source was used and applied to the walls of the tunnel system in the vicinity of the block. The measurements were carried out as vertical seismic profiling (VSP) and as horizontal seismic profiling (HSP) measurements. In the subsequent interpretation the results of the previous seismic investigations were taken into account.

5 Hydraulic model

During the past year, a study of the hydraulic data has produced a conceptual model of conductors and connections within the studied block. This study has only used pressure responses during drilling and interference test data to create the model. This work provides a purely hydraulic interpretation without bias from the geological and geophysical data, or the existing structural model. The hydraulic model identifies the connections that the structural model should explain, and serves as a basis for identifying anomalies or discrepancies that should be addressed in future testing or interpretation work.

5.1 Pressure and flow data during drilling

The analysis identified flowing features based on observations of inflow changes during drilling of KA2563A, KA3510A, KI0025F and KI0023B (it should be mentioned that some structures in KA2563A and KA3510A were grouted). The intersections with the flowing features were then correlated to the pressure responses in monitoring intervals in the borehole array. These correlations indicated which flowing features were part of common conductors or fracture networks. The hydraulic connections have been evaluated based on the 1) the geometric pattern of responses and 2) the strength of responses with respect to both the magnitude of drawdown and the speed the responses (diffusivity).

Using the pressure response data, a number of conductors with a high hydraulic conductivity compared to the surrounding rock, and with consistent distance-drawdown relationships have been identified. Three main types of distinct conductors were identified from the analysis:

1) A near-collar, major NW zone readily identified in all boreholes (including KA3510A, KA3573A and KA3600F). The width of this zone is in the order of tens of metres as shown in Figure 5-1.

2) Three well defined discrete conductors traceable between KI0023B, KI0025F and KA2563A. Figure 5-2 shows the responses to drilling KI0023B.

3) One isolated conductor connecting the bottom of KI0023B with the bottom of KA2511A.

In addition to these inferred conductors, a conductive feature appears to provide hydraulic connections along the length of KA2511A. The shallowest zones of this hole respond strongly to the near-collar conductive interval described above, and this response propagates rapidly to all the intervals of KA2511A. Subsequent to this initial

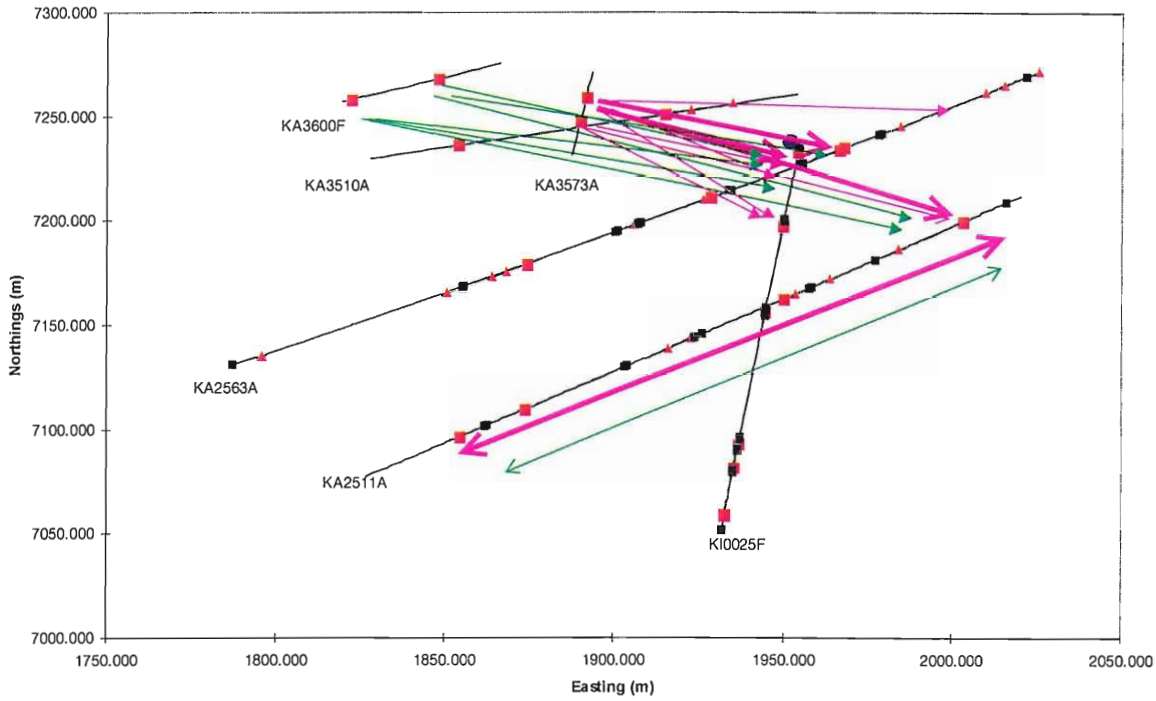

Figure 5-1 Visualisation in the horizontal plane of near-collar hydraulic connections and conductors interpreted from pressure responses observed during drilling of borehole KA3600F and KA3573A . This figure illustrates connections in the shallow, near-collar conducting zones. The solid green and purple lines correspond to the observed strongest hydraulic connections. N.B. the difference in horizontal and vertical scale.

"hit", all of the intervals of KA2511A have similar pressure responses. Furthermore, the hole does not appear to respond to drilling interference responses from other conducting zones, except for a strong connection to KI0023B in a conductor at the respective bottoms of these holes where they are closest.

5.2 Hydraulic model based on interference tests

A total of nineteen interference tests provide further information on the locations and connectivity of the conducting features in the TRUE Block Scale volume. Six of these tests had durations of 24 hours or more, and the remaining tests ran for approximately 30 minutes of pumping each. Preliminary analyses of these tests consider both

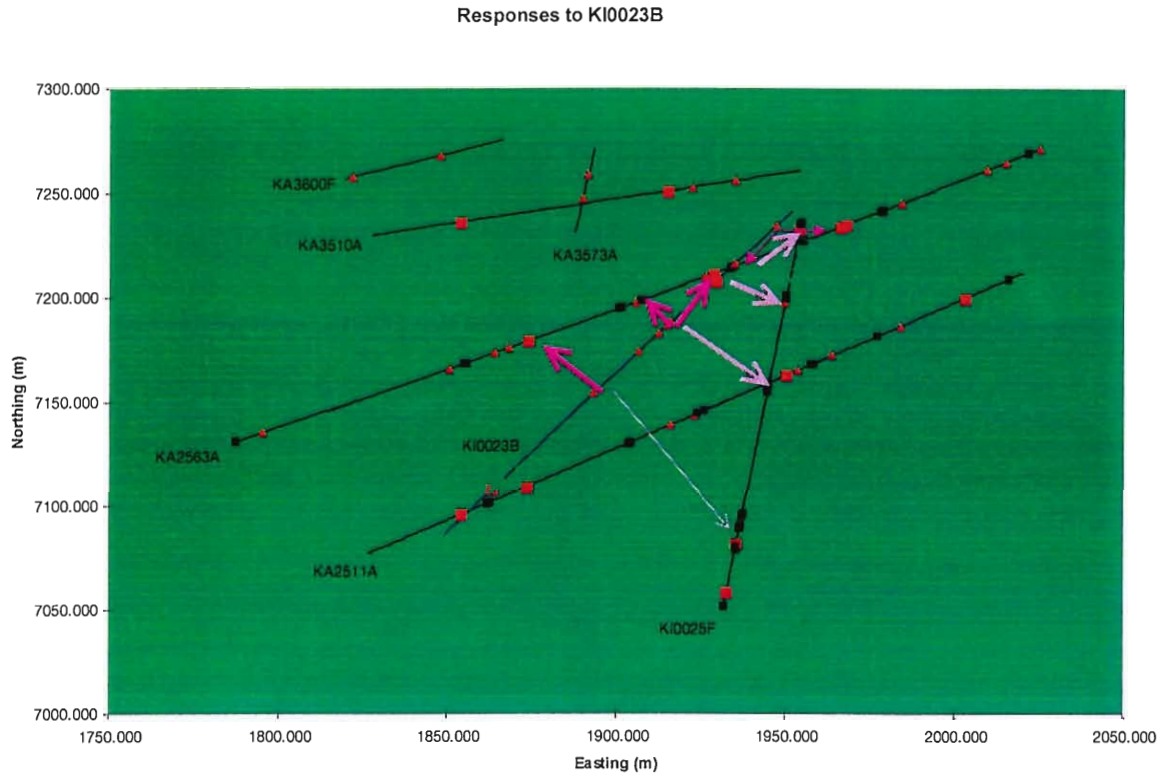

Figure 5-2 Visualisation in the horizontal plane of intermediate depth and deep-seated conductors interpreted from the analysis of pressure responses observed during drilling of borehole KI0023B. The solid purple and green lines correspond to the observed strongest hydraulic connections. N.B. the difference in vertical and horizontal scale.

drawdown and time to pressure response as complementary measures of connectivity. Comparison of drawdown from the pumping to the observation intervals is an obvious measure of connection, but it may be dependent on the network geometry and boundary conditions for the individual conductor. For example, any monitoring interval along a dead-end (i.e. terminates in a no-flow boundary), will tend to have strong drawdowns, even approaching those of the pumping well. Another measure is the time lag of the pressure response. This time lag is related to hydraulic diffusivity, and unlike drawdown, is relatively insensitive to flow geometry.

Figure 5-3 shows a conceptual model of major connections within the investigated rock volume. This model generally agrees well with the patterns of responses that were observed during drilling, cf. Section 5.1. The green lines connect the strongest

responding intervals, and define three conductors in addition to the shallow conducting interval. These are the same conductors that were identified using the pressure responses to drilling. The deep conductor in KI0023B was not tested.

The major conductors in Figure 5-3 are not the only connections in the block, but simply represent the strongest connections based on drawdown and diffusivity. The shallowest of the three conductors is well connected to the shallow conducting interval, while the deeper two conductors are relatively isolated. Furthermore, the plan view tends to emphasise steeply dipping conductors over gently dipping features. Nonetheless, any dominance exerted by subhorizontal features would tend to obscure the strong NW-SE anisotropy noted in the pattern of pressure responses.

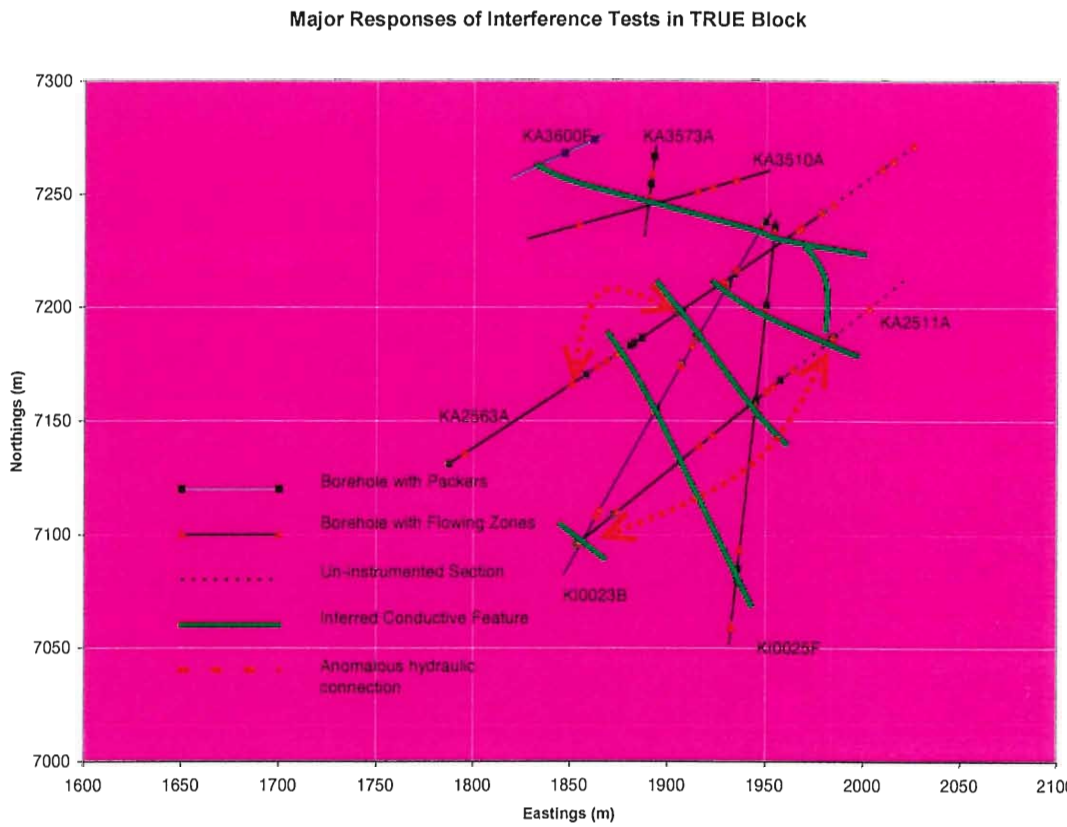

Figure 5-3 Hydraulic Conceptual Model of the TRUE Scale rock volume based on pressure interference tests. Please note that the conductor at the bottom of KI0023B is based on drilling responses, as there were no interference tests run on those intervals. Also the location of the deepest conductor in KA2563A is based on drilling responses as this interval of the borehole was not instrumented during the pressure interference tests. The solid green lines correspond to the observed strongest hydraulic connections. The hatched red lines indicate observed anomalous hydraulic connections.

In addition to the conductors described above, Figure 5-3 identifies two, anomalous hydraulic connections featured by highly diffusive connections between non-adjacent monitoring intervals of the same hole. Pressure transmissions along an anomalous hydraulic connection must jump monitoring intervals and other conducting features. The anomalous hydraulic connection along KA2511A was noted and discussed above under the section dealing with the responses to drilling. Its pressure responses tend to jump the second interval in KA2511A to create a response at the bottom of the hole.

An additional anomalous hydraulic connection appeared during the interference testing between monitoring intervals R1 and R5 in KA2563A. This connection is very strong, as interval R1 (numbering from the bottom of the hole) has nearly the same drawdown as interval R5 with little time lag. In short, sections connected by the anomalous interval respond as though they were very close despite the actual separation distance. Equipment or borehole effects have been considered among the possible explanations for anomalous hydraulic connections. While such effects are currently considered unlikely, further tests of the equipment may be devised to provide confirmation of equipment performance.

6 Structural model

The latest version of the structural model, the September 1998 model, uses characterisation data from all boreholes, including KI0023B. The September 1998 model also uses the results of the 1997/1998 three-dimensional seismic investigations as well as the results of the spring 1998 hydraulic cross-hole interference tests.

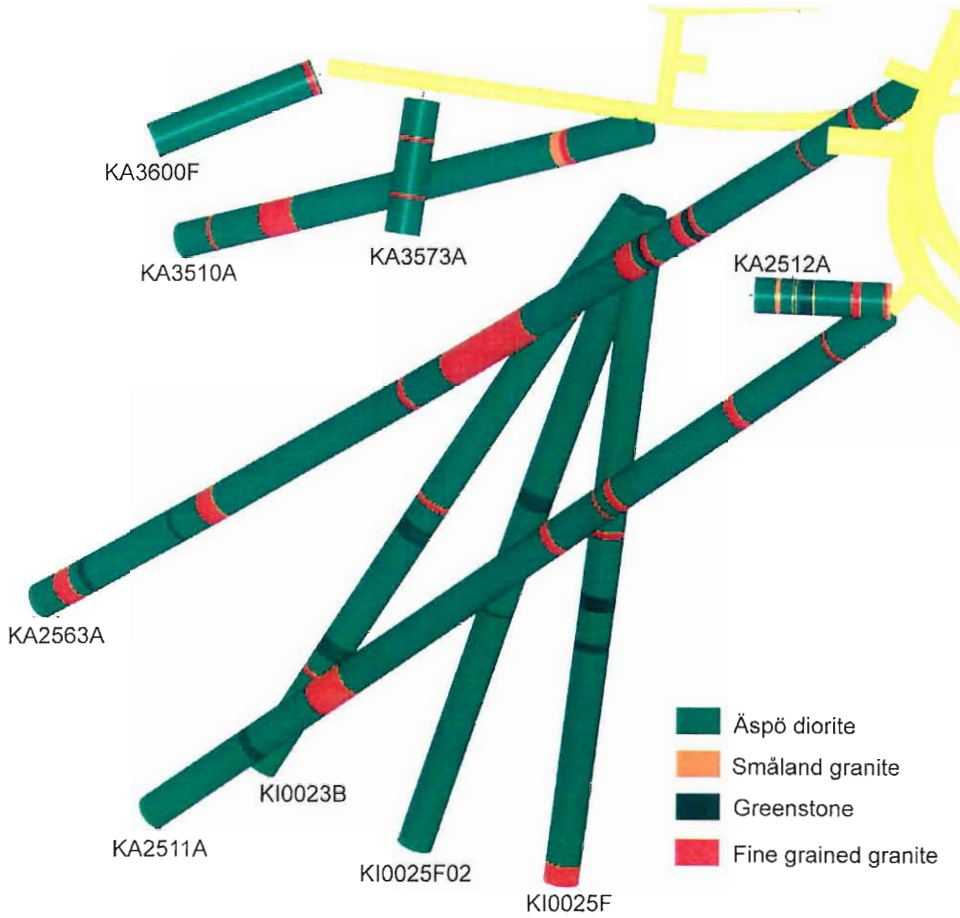

Figure 6-1 Plan view of lithology mapped from the cores of the boreholes sampling the TRUE Block Scale rock volume.

6.1 Geology

The lithology of the studied block is dominated by Äspö Diorite (86%). The diorite is also intersected by a number of fine-grained granite and a few greenstone bodies. The proportion of fine-grained granite is 12%, greenstone 1% and pegmatite <1 % is similar to the general picture in the Äspö HRL, the exception perhaps being a somewhat lower greenstone proportion compared to the generally observed 4-5%. The central area of the investigated block is intersected by a group of sub-horizontal aplites (fine-grained granites) of variable thickness and of variable extent. There are indications of greenstones occurring in conjunction with some of the aplitic bodies. The distribution of the lithological units is visualised in Figure 6-1.

Fracture orientations in all boreholes can be subdivided into three fairly well defined sets, steeply dipping NW and NNE trending sets and a sub-horizontal set. The sub-horizontal fracturing is most pronounced in KA2511A, whereas few sub-horizontal fractures are intersected in KI0025F and KI0023B as seen in Figure 6-2. Note that the apparent orientation in Figure 6-2 is influenced by a bias in orientation, which originates from sampling the 3-D network with a linear object such as a borehole. The total number of potentially conductive fractures in the boreholes is estimated to between 200 and 400 fractures (5-10% of all mapped fractures).

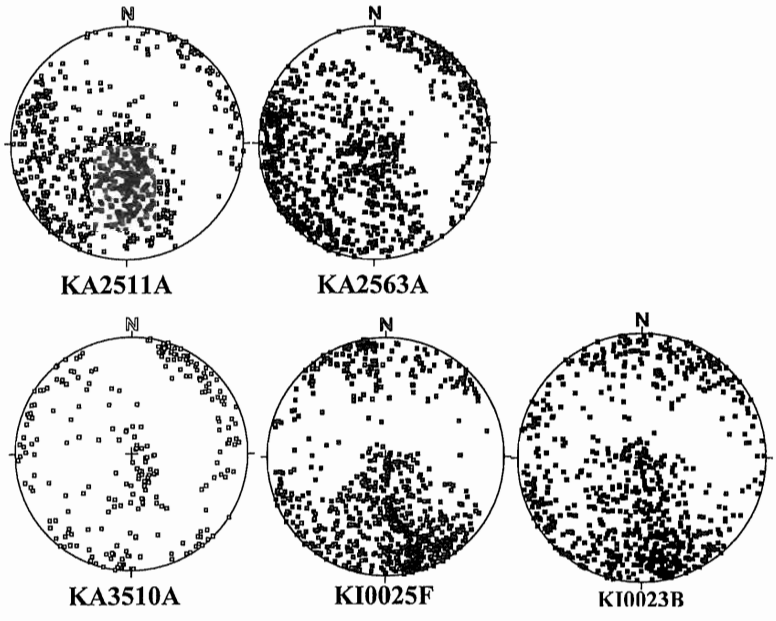

Figure 6-2 Fracture orientations observed in the cored boreholes penetrating the TRUE Block Scale rock volume (Poles of fracture planes projected on the lower hemisphere).

Table 6-1 Structural classification employed in developing the September 1998 structural model.

Fracture	Intercept of fractures without apparent shear or slip marks on fracture surfaces. No ductile precursor.
Fault	Visible shear or slip marks. Ductile precursor. The faults often have subparallel fractures, brecciation and cataclasis
Swarm	A large number of discontinuities which do not occur densely enough to qualify for the Zone concept. No crush in the drill core.
Zone	Intercept that occur as a large number of open faults and fractures over a short distance in the BIPS log, and as crush in the drill core. Heavily altered and deformed rock.

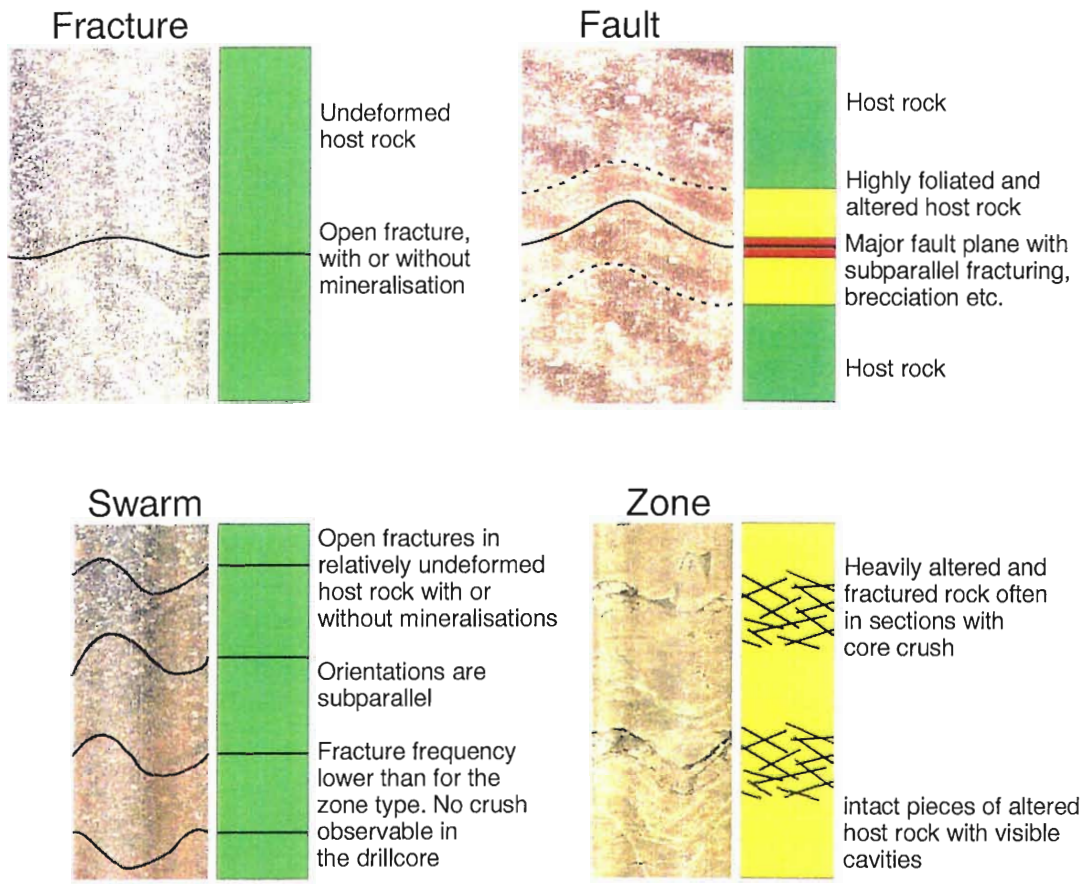

Figure 6-3 Examples of the identified intercept types of geological structures used in classification; A) single fracture, B) single fault and C) swarm of fractures, D) fracture zone.

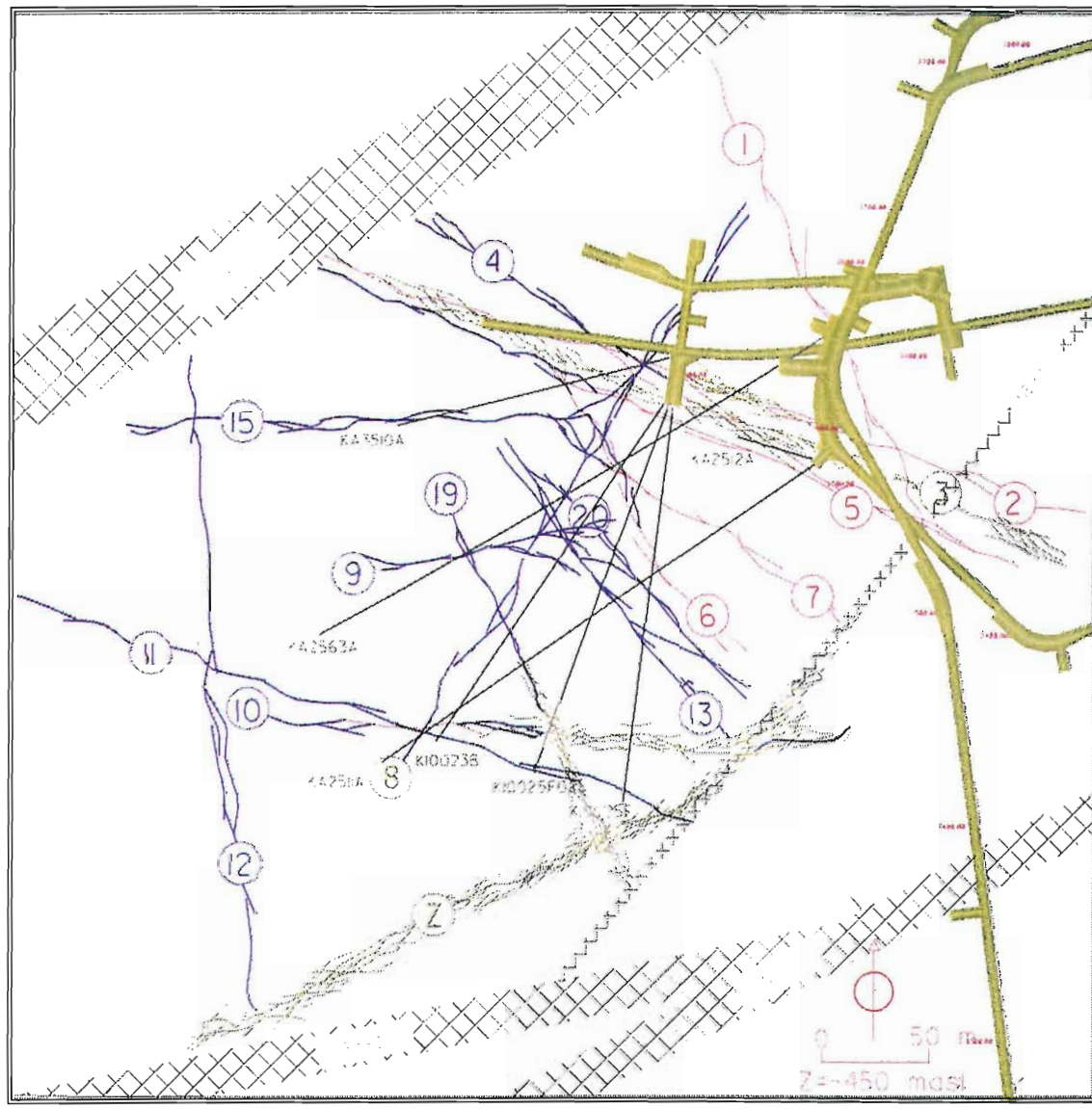

Figure 6-4 *Plan view of Sep'98 structural-geological conceptual model of the TRUE Block Scale rock volume. With reference to Table 6-1, the colour red represent a single fracture, blue a single fault and yellow a fracture zone. Swarms of fractures do exist but are of limited extension.*

6.2 Classification scheme

A geologically based scheme with four types of structures observed in core or borehole wall rock has been introduced. This categorisation is a valuable means to carry out the structural interpretation, and constitutes an important step introduced in the most recent structural model update. The four geological structure types are single fractures, single faults, swarms of fractures and fracture zones, cf. Table 6-1 and Figure 6-3.

6.3 Structural model

The September 1998 structural model is presented in Figure 6-4. This model employs the new classification scheme to present the model in a geologically more realistic fashion. The structural heterogeneity of many structures is emphasised by the use of the structural classification scheme. The observed geological heterogeneity can be directly related at places to the hydraulic information, cf. Section 7.1.2. Of particular interest is the interpreted variability of Structure 19 along its extension through the block. With the representation of the structural model in Figure 6-4 it should be emphasised that most of the structures are interpreted as narrow groups or networks of faults or fractures, rather than single fault planes. Although the geological character is emphasised in the visualisation of the model, it should be noted that when a structure is interpreted in a number of boreholes, the simplest assumption of planar extension has been taken in search for similar geological structures and/or hydraulic information in neighbouring boreholes. However, the experience is that geological structures at Äspö HRL are found to be heterogeneous in their lateral characteristics, resulting in intercepts with varied geology and also a varied hydraulic behaviour.

The overall structural pattern observed in the TRUE Block Scale rock volume is in line with what is observed on a site scale in the area bounded by fracture zones EW-1 and EW-3 and NE-1.

The individual structures are also supported by hydraulic. A breakdown of the supporting data for the respective interpreted intercepts is found in Appendix B.

It should be emphasised that an update of the structural model is presently under way where the results of the characterisation in KI0025F02 will be used to strengthen the interpretation of the structures in the central part of the investigated block.

7 Groundwater flow

The characterisation of groundwater flow in the TRUE Block Scale rock volume requires an understanding of how water flows under natural conditions. With this knowledge as a basis we are in a position to make projections of what will happen when we disturb the system at a given location and with a given amount. This understanding is paramount for making projections of the success of planned tracer tests in the block scale. It should however be understood that data for understanding natural groundwater flow come from tests performed under stressed conditions. Given that the block is located in the immediate vicinity of a major underground laboratory the term "natural" should in this context be regarded as relative.

In order to identify the pattern and control of natural groundwater flow at the scale of the investigated block we need to know three basic elements; 1) the geometry and connectivity of the network of conductive elements, whether made up of structural or lithological elements, 2) the hydraulic conductivity or transmissivity of these elements, and 3) the boundary conditions acting on the block of interest.

The following sections present an analysis of the data and the current conceptualisation of the groundwater flow through the block.

7.1 Basic background information

7.1.1 Geometry and connectivity of conductive elements

In Chapter 5 it was shown independently from any other structural or geological data that four main north-westerly oriented conductors dominate the connectivity of the investigated block: (1) a major zone NW zone near the collars of the boreholes, (2) a single conductor at L=70 m in KI0023B, (3) a conductor at L=40 m in KI0023B, and (4) a conductor at L=112 m in KI0023B.

A comparison with the structural model presented in Chapter 6 reveals that conductors 1) through 3) coincide with interpreted structures, specifically: (1) a group made up of Structures #1-5, (2) a group made up of Structures #13, #9 and primarily Structure #20, and (3) Structure #7, respectively. Conductor 4) appears to correspond to Structure #19, and is relatively hydraulically isolated. This structure constitutes the principal upstream boundary to the area of interest.

The spring 1998 interference tests identify Structure #1 and #5 as high-transmissivity structures. The former is not considered important for the hydraulic behaviour of the block. Structure #5 exhibits a high transmissivity throughout its extent and constitutes a

well-defined boundary. Structure #7 is likewise a high-transmissive feature, with a good connectivity to Structures #5 and #15. The response pattern of the tests in Structures #5 and #7 are the same, ie. they respond jointly. Structure #20, which is less transmissive than Structures #5 and #7, on the other hand, exhibits moderately high connectivity within the interpreted structure. This feature is well connected and responds jointly with Structures #9 and #13, but differently compared to the group made up of Structures #5 and #7 above. The block seems to host one "global network" made up of Structures #5, #7 and one "local network" made up of Structures #9, #13 and #20, and possibly Structure #6. Structure #19 constitutes a bounding upstream structure, relatively isolated from the two defined networks of structures.

The spring 1998 interference tests do not provide any evidence, direct or indirect, of the existence of a subhorizontal set of structures. It should however be stated that the seismic work does show an indication of a subhorizontal structure below the borehole array, gently dipping to the east slightly below an elevation of –450 masl.

Table 7-1 provides a comparison between a graded assessment of connectivity within the block as obtained from the cross-hole interference tests and the geometrical connectivity established by the September 1998 structural model. In some cases the structural model would predict connections in places where no hydraulic connection has been observed. Such a situation may result from 1) heterogeneity within a given structure, or 2) the structure is in fact not being made up of one plane, but of two or more which may not necessarily be fully interconnected. The constructed matrix in Table 7-1 should be viewed as a tool for keeping track of the three-dimensional connections which develop below and above the reference datum for the structural model visualisation which is located at Z=-450 masl, cf. Figure 6-4.

The interference tests that have been performed as part of the characterisation in the new borehole KI0025F02 will be instructive for verifying or improving the assessment of the geometry and interconnectivity of the identified structures.

7.1.2 Material properties

The hydraulic tests show a wide range of transmissivity for the interpreted structures in the investigated block. These range from values at the limits of measurement ($< 5 \cdot 10^{-10}$ m^2/s) to values in the order of $5 \cdot 10^{-5}$ m^2/s, i.e. a span of 5 orders of magnitude. Also in the case where a number of intercepts for a given structure has been tested in different boreholes, the variability in some cases is high. This finding supports the element of the conceptual structural model discussed in Chapter 6, which features variability in geological and structural characteristics along the extension of some interpreted structures, which in turn may entail similar variability in hydraulic properties.

Table 7-1 Comparative connectivity matrix – Comparison between an assessment of hydraulic connectivity (colours) inferred from performed interference tests and the geometrical connectivity established from the September 1998 Structural Model (crosses).

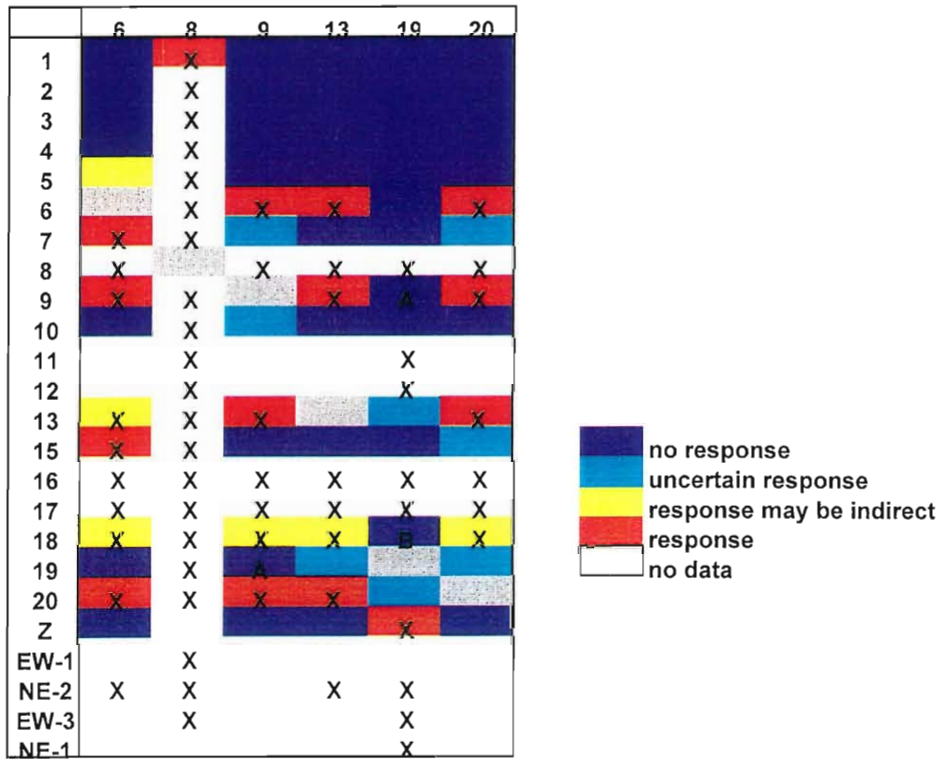

Recent analysis of the interference tests and single hole transient flow and build-up tests has indicated that the transient evaluation is affected by constant head boundary effects. In the case of evaluation of the responses, the existence of a constant head boundary may lead to an overestimation of the transmissivity. Preliminary results indicate that the local network of fractures made up of Structures #9, #20, #13 (possibly including Structure #6) have a transmissivity below $7 \cdot 10^{-7}$ m^2/s.

Table 7-2 summarises the available transmissivity data attributed to the structures of particular interest in the TRUE Block Scale rock volume.

Table 7-2 Ranges of transmissivity (m^2/s) obtained for interpreted structures from different characterisation techniques (Sep '98 model).

Structure	Double packer flow logging (5m)	Transient flow and pressure build-up tests	Interference tests (observ. section)	Interference tests (source section)
#5	No data	No data	$2\cdot10^{-5} - 4\cdot10^{-5}$	$1.5\cdot10^{-5}$
#7	$5\cdot10^{-8} - 2.6\cdot10^{-6}$	$9.9\cdot10^{-7} - 1.8\cdot10^{-5}$	$2\cdot10^{-5} - 5\cdot10^{-5}$	$2.4\cdot10^{-6} - 4.3\cdot10^{-5}$
#6	$7\cdot10^{-8} - 1.5\cdot10^{-6}$	$6.4\cdot10^{-9} - 4\cdot10^{-7}$	No data	No data
#20	$1.2\cdot10^{-9} - 3.8\cdot10^{-7}$	$4.7\cdot10^{-8} - 7.9\cdot10^{-7}$	$7\cdot10^{-7} - 1\cdot10^{-6}$	$8.1\cdot10^{-7} - 1.5\cdot10^{-6}$
#9	$4.6\cdot10^{-8} - 1.3\cdot10^{-7}$	$3.5\cdot10^{-7} - 8.4\cdot10^{-7}$	$7\cdot10^{-7} - 1.2\cdot10^{-7}$	$1.2\cdot10^{-6}$
#13	$2.8\cdot10^{-8} - 3.1\cdot10^{-8}$	$5.8\cdot10^{-8} - 9.8\cdot10^{-8}$	No data	No data
#19	$2\cdot10^{-10} - 7.3\cdot10^{-7}$	$2.7\cdot10^{-7} - 1.2\cdot10^{-5}$	No data	No data

7.1.3 Boundary conditions

The hydraulic heads acting on the boundaries of the block define the driving forces for groundwater flow and largely govern the flow pattern within the block. The source for information on the boundary conditions can be either direct or indirect. The direct information stems from measurements of groundwater pressure in the measurement intervals isolated by the multi-packer systems in the exploration boreholes. Relatively calm time periods when the pressure is largely unaffected by activities in the laboratory can be used to infer "undisturbed" boundary conditions, and can also be used to infer hydraulic gradients on a local scale. In this context it should be mentioned that the tidal effects at Äspö are ∀ 2 kPa.

The source for indirect information is the existing numerical models of the Äspö site which have been developed over the last couple of years. Svensson [4] has presented a model of the site that is based on the most recent site-scale structural model [5]. This model has been calibrated against available data before tunnel construction, and also following tunnel construction, including drawdown data from performed pump tests and inflow to the tunnel. A relatively good agreement is presented for this model between calculated and measured responses, both without and with the Äspö HRL in place. For the area of the model where TRUE Block Scale is located, a gradient of approximately 10 % is observed directed towards the north-east, the magnitude being in parity with what has been measured (along the boreholes) in the interior of the TRUE Block Scale rock volume. In addition the model show an upward component of flow in the area of

the TRUE Block Scale volume. These two observations show the control exerted by the spiral tunnel and the existing shafts. Data from the Svensson 1997 model has been used to extract boundary conditions for the ongoing discrete fracture network and stochastic continuum modelling.

The constant head boundary effects that have been observed to affect the evaluation of transmissivities can be interpreted in two ways. First, the boundary effect may be the result of a connection of the tested fracture to a high-conductive fracture. This is also in line with the leaky aquifer model inferred from the cross-hole interference tests perform3ed during the Spring 1998. The second possibility is that flow becomes three-dimensional in a well-connected fracture network away from the borehole section.

7.2 Description of groundwater flow

7.2.1 Participating conductors

The investigated block is bounded upstream by Structures #10, #11 and #19, and downstream by Structures #1-#5. The block is flanked in the north-west by Structures #12 and #15, respectively. In the south-east the flanking structures are Fracture Zone Z and the site scale Fracture Zone NE-2.

The conductors of primary interest to the project, which are interpreted to participate in groundwater flow in the block, are Structures #19, #13, #20, #9, #6, #7 and #5. Possibly, parts of Structure #8 participate in flow. Although results from the interference tests did not reveal any evidence of participation of a subhorizontal set of structures, it cannot be ruled out they may play a partial role. It should be remembered that the seismic work does show evidence of subhorizontal structures but below the borehole array, cf. Section 7.1.1.

The geometries of the structures are given in Chapter 6 and Appendix A. The transmissivities are presented in Section 7.1.2.

7.2.2 Flow directions on a larger scale

As mentioned in Section 7.1, the major control of natural groundwater flow in the block is exerted by the tunnels and shafts. In the TRUE Block Scale rock volume this results in a dominating driving force for flow directed towards the northeast. An assessment of the hydraulic head situation can be made by revisiting the hydraulic head data that were collected prior to onset of the interference tests performed in the Spring 1998. Typical hydraulic head values for Structures #19, #20, #6, #7 and #5 can be inferred from the data. These typical values are shown in Table 7-2, and represent a breakdown of available head data as presented in Table 7-3.

Table 7-2 Average values of hydraulic head (April 8, 1998) attributed to defined structures.

Structure label	Hydraulic head (masl)
#19	-25.8
#20	-28
#6	-31.8
#7	-35.4
#5	-39.1

From the head data presented in Table 7-2 it is possible to estimate a gradient across the block (Structure #19 towards Structure #7/#5). This gradient amounts to about 8-9 % and is in parity with what is observed in the interior of individual exploration boreholes. In addition this gradient is consistent with what is observed in the modelling results presented by Svensson [4]. The relatively high head in Structure #5, which is located close to the lower part of the TBM tunnel, is in parity with the low inflow of water observed to the TBM tunnel.

It should, however, be noted that given the anisotropic nature of the hydraulic properties of the block, the actual flow pattern is more intricate, and it is governed by the relative transmissivities of the existing structures. It is well known from previous studies at Äspö that the northwest fracture system and structures are more transmissive [5]. This is also supported by the rock stress situation, with the maximum principal horizontal stress oriented northwest [6]. It should also be noted that the hydraulic model presented in Section 5.2 supports the observed hydraulic anisotropy.

7.2.3 Groundwater flow in network of structures

The structures discussed in Section 7.2.1, which are of primary interest to the project, are Structures #19, #13, #20, #6, #7 and #5. Table 7-3 reports the measured hydraulic heads in sections containing these structures prior to the start of the interference tests. An assessment of the direction of flow in these structures can, in principle, be assessed from local measurements of hydraulic head. With the knowledge of the location in space of the measurement intervals it is possible not only to make a rough qualitative estimate of the direction of the lateral gradient (flow direction), but also to assess the direction of the vertical component of flow.

Table 7-4 provides a summary of the inferred direction of flow in the given structures as determined from two-point values selected from Table 7-3. Head values from sections that are interpreted to contain two or more structures have not been utilised in the inference of flow direction (Table 7-3 and Table 7-4). The values from monitoring intervals with more than one structure stand out as anomalous compared to the values which contain a single intercept of the structure in question. The inferred flow directions in interpreted structures are also presented in Figure 7-1. **It should be emphasised that the inferences made regarding flow directions are based on a limited data set, for the most part only supported by two useful measurement points in a given structure. In addition the data constitute only one point in time. The inference should thus be regarded as preliminary and associated with some uncertainty.**

The flow directions inferred from head data are prevailingly directed along the north-westerly structures towards the north-west, cf. Figure 7-1. The head data presented in Table 7-2, suggests that the north-westerly structures are connected and the block is drained towards the end of the TBM tunnel (Prototype Repository). This connection of the north-west trending set of structures can be established either by the interpreted Structure #8, or alternatively by subhorizontal structures, or by diffuse background fracturing (fracture network). The results of the performed interference tests show no hydraulic evidence, either of Structure #8, or of subhorizontal structures. It should however be pointed out that this inference is based on the available borehole intercepts. It cannot be ruled out that Structure #8 does connect the structures oriented north-west. Notwithstanding how the north-westerly structures are connected, we do know that the transmissivity of the connecting elements is substantially lower than in the north-westerly structures. Again, this inference of hydraulic anisotropy is substantiated on a site scale by previous observations at the Äspö HRL [5].

The modelling performed within the project using Stochastic Continuum techniques includes the interpreted structures in their correct locations. Alternative transmissivity characteristics and correlation structures are accounted for in the structures and the rock matrix, respectively. The model has been conditioned to measured transmissivity and inversely to measured steady-state head. The model results are hence conditioned to the steady state head which have been used in the preceding section to infer the flow pattern. Notwithstanding this fact, the modelling results fill in the gaps in the picture of groundwater flow, cf. Figure 7-1. The south-east parts of Structures #19, #13 and #7 are all featured by a flow direction towards the north-west. The north-western parts of Structures #19 and #13 both exhibit a reversed flow direction, due south-east. In the

north-western part of Structure #7 and in Structure #6 the flow direction is orthogonal to the structures, due north-east, and towards the tunnels. Structure #9 shows flow along its extension towards the east, whereas no clear flow direction is evident in Structure #20.

A comparison between the flow directions derived from the stochastic continuum modelling with those based on head data, overall show a good correspondence.

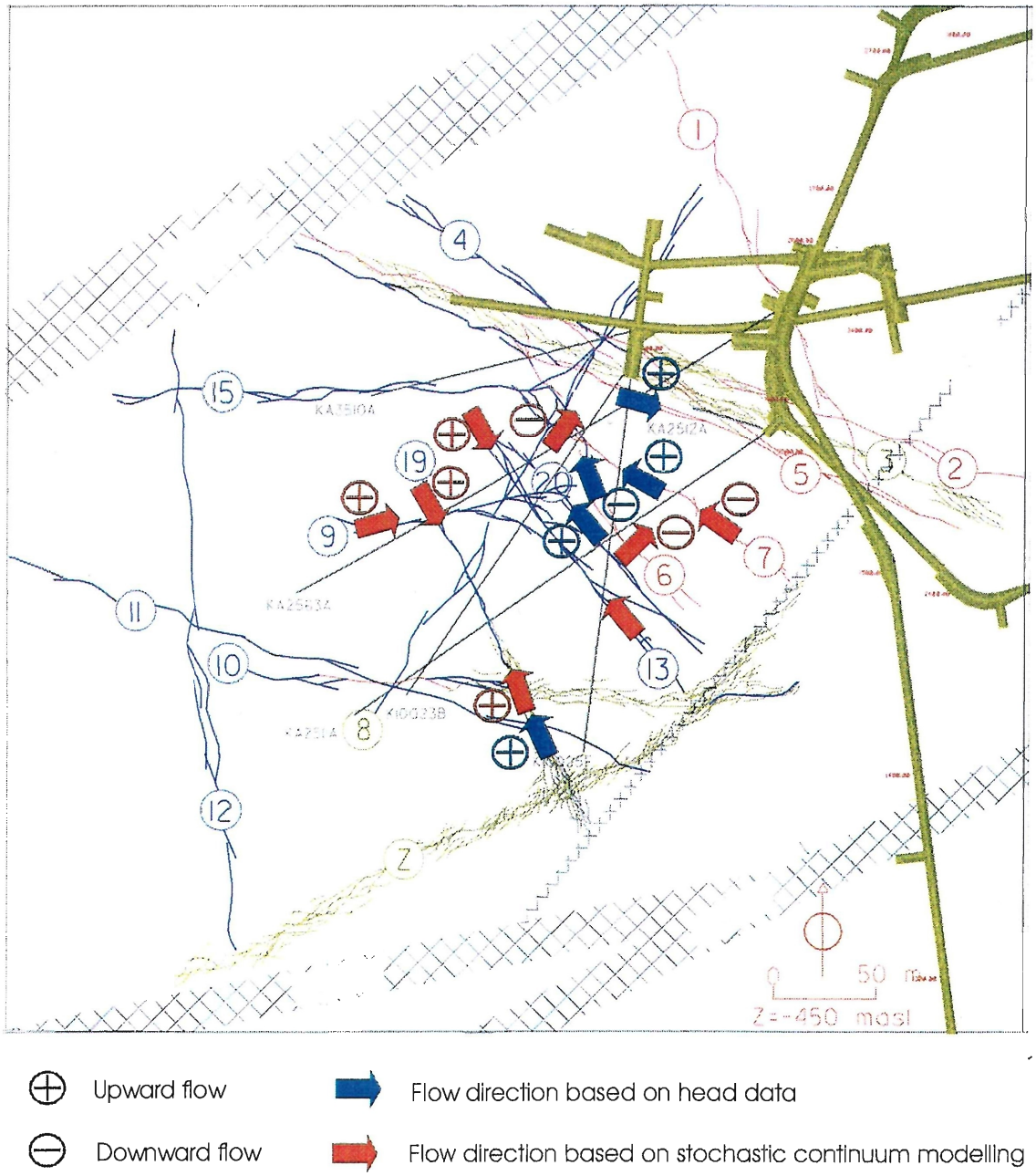

Figure 7-1 Plane view of groundwater flow directions inferred from analysis of hydraulic head data and stochastic continuum modelling.

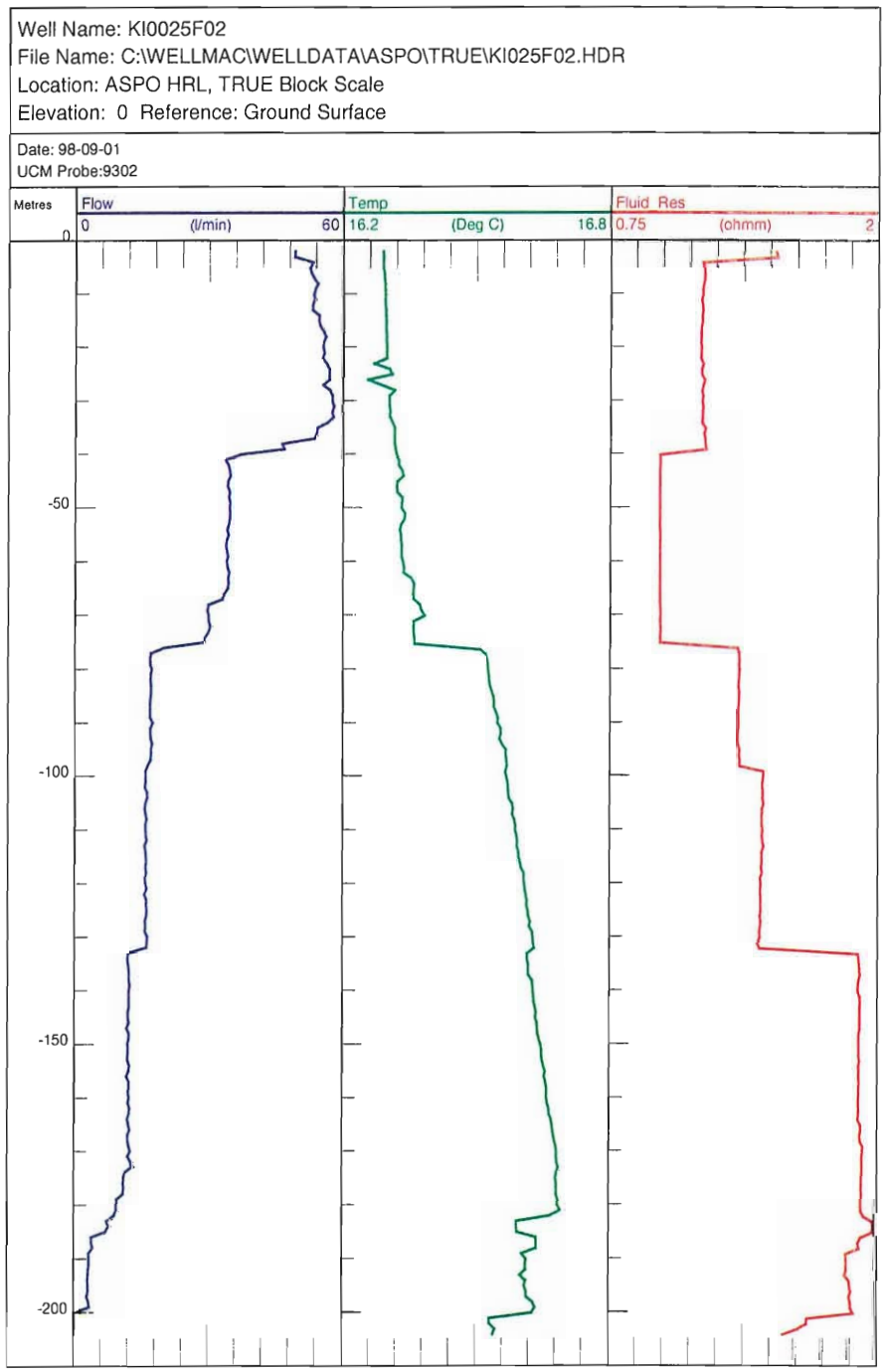

Figure 7-2 Example of a UCM acoustic flow log from borehole KI0025F02 complemented by temperature and fluid resistivity log.

A variation in the inferred vertical component of flow is observed, cf. Table 7-4, with a downward component in the interior of the block and an upward component in Structures #5, #19 and Structure #20. The latter observation is consistent with the modelling results presented by Svensson [4]. The Stochastic Continuum modelling performed shows a prevailing upward component of flow in Structures #19, #9, #13 and #20. Structures #6 and #7 show downward flow. The results of the Discrete Feature Network modelling suggest upward components of flow in Structures #7, #19, #20, #6 and #5.

It should be noted that the acoustic flow meter measurements (UCM) are complemented by simultaneous measurements of fluid resistivity and temperature. These logs are available for all the long boreholes (N.B. the tool is moved from the bottom of the hole and upwards). These logs can be used to assess the vertical component of flow in the interpreted structures. The suite of logs from KI0025F02, cf. Figure 7-2, show that Structure #7 (at 40 m depth) shows inflow of water with a fresh-water signature (increased resistivity), suggesting inflow ofless saline water from the structure into the borehole, possibly suggesting downward flow (recharge conditions). A contrasting result from Structure #20 at approximately L=75 m depth shows inflow of a more saline water reducing the fluid resistivity, and suggesting an upward flow component in this structure at this depth. However, surprisingly enough, the temperature log shows a reduction at this depth. The difference in resistivity and temperature signatures between the interpreted structures in the borehole also provides support for the relative separation between the northwesterly oriented structures, cf. Section 7.1.1.

An evaluation of the limited chemical data available from the instrumented boreholes indicates that the sections containing the constituents of the near-collar Structures #1 through #5 and Structure #6 contain Baltic Sea water. This observation suggests a downward flow component, cf. results of chemical analyses in Appendix C. The Baltic Sea water is characterised by high ^{18}O-values (approximately –7 ‰) and low concentrations in chloride (3000-4000 mg/l), and high concentrations of magnesium. This set of zones is interpreted to connect to fracture zone EW-1, cf. Figure 6-4. However, available chemical data show no evidence of Baltic Sea water in the waters sampled in EW-1 during pre-investigations. It is therefore proposed that the apparent Baltic Sea waters are derived from the package of fracture zones made up of NE-1, EW-3, NE-1 and Z.

The chemistry of the waters observed in Structures #9, #20 and #7 shows evidence of a mixture of Brine-Glacial-Meteoric where the glacial component is expected to be small and the meteoric component is successively fed to the system. It should however be emphasised that a Baltic Sea water component is observable, but subordinate. This type of water is typical for this depth at Äspö HRL and is characteristic of compartments bounded by structures where Baltic Sea water recharge occurs. In some cases, samples from Structures #20, #13 and #19, the high chloride and low carbonate concentrations even suggest upward flow of more deeply derived waters.

7.2.4 Magnitude of hydraulic gradient and groundwater flow

Table 7-4 also reports the magnitude of the hydraulic gradient as inferred from the analysis of available head data. The hydraulic gradients inferred using head data from the structures span from 0.01 % to 2.8 %. The lowest gradients are noted for the high-conductive structures, #7, #6 and #20. The highest gradients are noted for Structures #5 and #19. **On the same grounds as for the discussion of flow directions, the calculated gradients should be regarded as preliminary and associated with some uncertainty since they are only based on two points in each structure.**

Also included in Table 7-4 are the results of performed point dilution. These gradients are backed out of the inferred Darcy velocities using a hydraulic conductivity assigned to the section in question. The measured Darcy velocities range from $1.8 \cdot 10^{-9} - 4.6 \cdot 10^{-7}$ m/s. The inferred gradient from the measured velocities is very sensitive to the hydraulic conductivity used in the calculation.

A comparison between the two-point gradients based on hydraulic head and the gradients based on point dilution data show that that a relatively good comparison is obtained for Structures #7 and #19, where the dilution-based gradients are within one order of magnitude higher than those based on head data.

In the case of Structures #6 and #20 the head-based gradients are within a factor 200 higher than those derived from point dilution data.

It should be noted that the inferred gradients, whether head-based or dilution-based, are associated with uncertainty. The results from the two methods should not be used separately, but jointly since the head-based values can be viewed as more "integrating" whereas the dilution-based gradient constitute "point values".

Using average calculated flows in the structures contained in the stochastic continuum model, 0.001 – 0.3 l/min, and average effective hydraulic conductivities, average hydraulic gradients have been calculated. The inferred gradients obtained for Structures #7, #13, #19 and #20, amount to 16, 2.8, 1.7 and 2.5 %, respectively. These values are comparable with calculations based on the measured head data. The inverse modelling procedure employed has resulted in low effective hydraulic conductivities for Structures #6 and #9, $K=8.3 \cdot 10^{-10}$ and $2.9 \cdot 10^{-9}$ m/s, respectively. As a consequence the calculated gradients are extremely high in these two structures, 20 and 5.7 m/m, respectively.

The results of the steady state calibrations based on the Discrete Feature Network modelling have been used to calculate hydraulic gradients in the interpreted structures. In these calculations, the calculated head in the corresponding sections used for the inference based on measured head data have been used. The calculated gradients for Structures #7, #19, #20, #6 and #5 are 7.5, 1.4, 0.9, 0.7 and 5.3 %, respectively.

Table 7-3 Compilation of undisturbed hydraulic head data from packed-off selected structures. Field data collected April 8, 1998.

Borehole section	Structure id.	Hydraulic head (masl)	Elevation of section (masl)
KA2511A:S5	#7	-35.41	-365.09
KA2563A:R6	#7 (#6)	-32.20	-451.81
KI0023B:P8	#7	-35.41	-462.60
KI0025F:R5	#7 (#6)	-35.36	-469.42
KA2511A:S3	#19 (#20, #17)	-30.68	-425.79
KA2563A:R2	#19	-	-491.33
KI0023B:P2	#19	-26.56	-487.66
KI0025F:R2	#19	-25.02	-501.23
KA2511A:S3	#20 (#19,#17)	-30.68	-425.79
KA2563A:R5	#20	-28.00	-466.56
KI0023B:P7	#20 (#6)	-29.61	-467.88
KI0025F:R4	#20	-27.99	-477.08
KA2511A:S4	#6	-31.47	-391.37
KA2563A:R6	#6 (#7)	-32.20	-451.81
KI0023B:P7	#6 (#20)	-29.90	-467.88
KI0025F:R5	#6 (#7)	-35.40	-469.42
KA2563A:R7	#5 (#4, #17)	-39.19	-414.77
KI0023B:P9	#5	-47.74	-455.68
KI0025F:R6	#5	-38.02	-455.72

Table 7-4 Inferred flow direction from hydraulic head data presented in Table 7-3. Calculated hydraulic gradient based on head data compared with hydraulic gradients inferred for interpreted structures from point dilution measurements.

Structure id.	Inferred flow direction (Head)	Hydraulic gradient (m/m) (Head)	Inferred vertical component of flow (Head)	Hydraulic gradient (m/m) (Point dilution)
#7	KI0025F 6 KI0023B	0.0001	Downward	0.0004
#19	KI0025F 6 KI0023B	0.018	Upward	0.01
#20	KI0025F 6 KA2563A	0.0002	Upward	1.2
#6	KA2511A 6 KA2563A	0.0091	Downward	1.6
#5	KI0025F 6 KA2563A	0.028	Upward	-

8. Prospects for future transport experiments

8.1 Background

The analysis of the potential for future tracer tests is based on a number of different inputs. The primary goal at this stage is the understanding of the structural model and its support from the hydraulic characterisation. This understanding is conveyed in Sections 6.3 and 7.1.1 and 7.2.3. The results of this integration show one global and one local interconnected network. The former made up of Structures #7 and #5 and the latter made up Structures #20, #9, #13, and possibly #6. The local network of connected structures has transmissivities less than $7 \cdot 10^{-7}$ m^2/s. In addition, a series of transport-related experiments were performed during 1998 to further elucidate the potential for performing transport experiments in the investigated rock volume.

During the interference tests, tracer dilution tests were performed in seven sections. These tracer dilution tests served three purposes, which are the following: 1) to complement the picture of pressure-based connectivity with one based on changes in flow in injection sections due to pumping, 2) to assess the potential for performing tracer tests with the applied hydraulic stresses and over the distances employed, 3) to produce a calibration data set for the modelling performed with various concepts.

During one of the interference tests (ESV-1c) the pumping in the source well was prolonged to also observe breakthrough of tracer injected in three sections in the borehole array.

It should be mentioned that the multi-packer system in borehole KI0023B has suffered a partial collapse in Section P3 (87.2-110.25 m) which is a low-conductive section ($T < 4 \cdot 10^{-9}$ m^2/s). This collapse was caused by an under-dimensioned pipe. The collapse caused a minor leak from the section amounting to 25 ml/min. Communication with the inner two test sections P1 and P2 is restored when a pressure of 2 bars is maintained in section P3. An attempt made to extract and repair the system failed because of a wedging rock fragment after moving the system some 17 metres. The system was instead returned back to its original position. In order to assess the implications of the partially failed system for future tests, a tracer dilution test was conducted to assess the effects of the reduced pressure and leakage. The results of this test show that the natural flow rate in Section P4 (Structure #13) is not affected. There exists a flow path for solute transport between section P4 and P3. This leaky passage is deemed insignificant based on the experimental results, so that the failed section will not have any serious effect on future transport experiments.

In conjunction with characterisation of the new borehole KI0025F02, complementary dilution tests have been carried out as part of the flow and pressure build-up tests, and after installation of a multi-packer system in the new borehole.

8.2 Results from interference tests

8.2.1 Tracer dilution tests

In total, 51 measurements of flow rate were made during the March-May 1998 interference tests using the tracer dilution technique both under undisturbed and stressed (pumped) conditions. The results show that only two sections respond significantly to the pumping, namely KA2563A:R5 (Structure #20) and KI0023B:P6 (Structure #9). A minor change in flow rate was also inferred for section KI0023B:P4 (Structure #13), the latter observation is however deemed highly uncertain.

The experience from the First TRUE Stage experiments on a single structure, performed in a separate part of the Äspö HRL, and on a detailed scale (< 5 m), shows that the success of a tracer experiment to a large extent rely on the possibility to establish a notable change of flow rate in the proposed injection sections.

Prior to performing the interference tests, the selection of the pumping rate had been carefully considered with an eye to reducing the effects of turbulence in high-conductive zones. Consequently, the source sections were not opened to atmospheric pressure conditions completely. Rather, the drawdown in the pumped sections was kept between 2.9 to 62 m. The one exception was the test ESV-1b where a drawdown of 415 m was established. The resulting pumping rates varied between 0.4 and 4.1 l/min.

In retrospect, a usage of atmospheric boundary conditions during pumping may have yielded a larger number of borehole intervals where the groundwater flow changed, thus providing a more complete picture of the transport-based connectivity and possibilities for future tests.

8.2.2 Tracer tests

Three injections of conservative dye tracers were made during the tracer test ESV-1c while pumping in KI0023B:P6 (Structure #9) at Q=1 l/min. The pumping in this zone was prolonged to observe breakthrough of tracer. One distinct breakthrough was obtained from injection in KA2563A:R5 (Structure #20). This breakthrough curve is shown in Figure 8-1. The mass recovery of this experiment was 44%. No breakthrough was observed for the remaining two injection in KI0025F:R4 (Structure #20) and KI0023B:P4 (Structure #13) over the duration of the experiment, which was 384 hours (16 days). The distance between the injection and pumping section varied between 15 and 42 m.

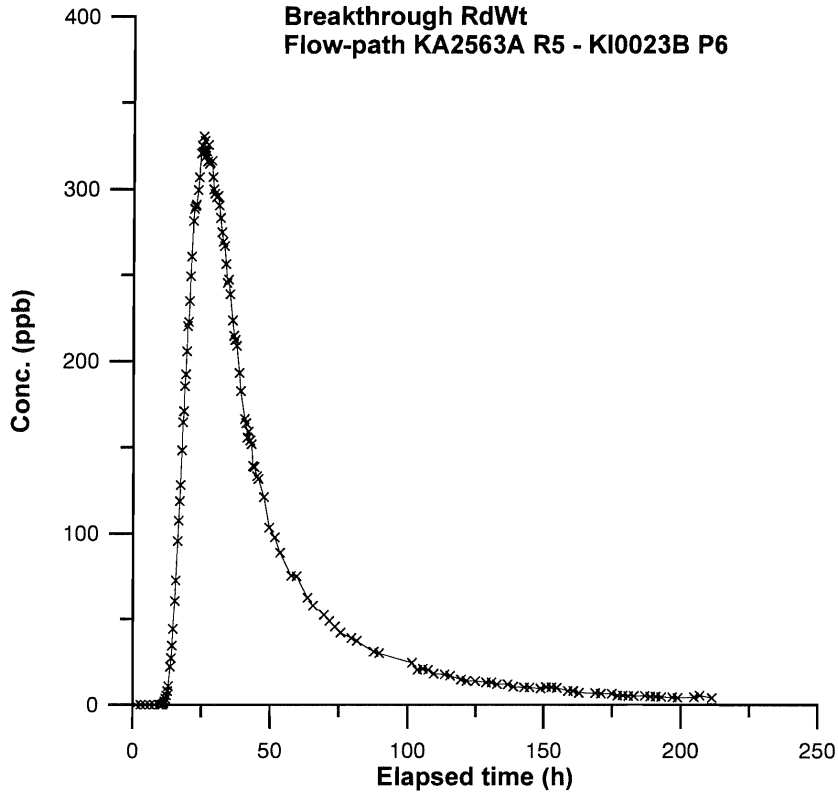

Figure 8-1 *Tracer breakthrough in KI0023B:P6 from injection of Rhodamine WT in borehole section KA2563A:R5 during interference test ESV-1c.*

The results of this experiment show that a tracer experiment can be performed successfully in the studied fracture network over a distance of about 16 m at the site of the TRUE Block Scale experiment. However the results also show that the fracture system needs to be stressed more to obtain breakthrough from multiple injection points. This was taken into account when performing complementary tests involving the new borehole KI0025F02, cf. Section 8.3.

Another means to improve tracer recovery is to apply a forced injection procedure (unequal strength dipole configuration, not applied here).

8.3 Results from tests involving KI0025F02

8.3.1 Background

The objectives of the performed tests have been to provide detailed information regarding the hydraulic characteristics of structures within borehole KI0025F02 which may be considered as boundaries to, or target features within, a delineated block for future hydraulic and transport experiments. The specific objectives of the tracer dilution

tests were to demonstrate the feasibility of performing tracer tests within specific test intervals in the new and existing boreholes. A secondary objective has been to provide information to optimise the configuration of the multi-packer system in borehole KI0025F02.

Two types of tests have been performed involving borehole KI0025F02. The first set of tests constituted pumping of two sections packed off with a movable double packer system in conjunction with flow and pressure build-up tests in KI0025F02, with simultaneous tracer dilution tests in three sections in neighbouring boreholes. The second set of tests, which are presently being evaluated, involved pumping in one section in KI0023B with simultaneous tracer dilution tests in three sections in the instrumented borehole KI0025F02. The two test campaigns to some degree test reversibility in transport in the investigated block.

8.3.2 Tracer dilution tests during build-up tests in KI0025F02

Tracer dilution tests were performed in three borehole sections associated with structures #9 and #20; KI0025F:R4 (#20), KI0023B:P6 (#9) and KA2563A:R5 (#20). The measurements were done during undisturbed conditions, and during pumping at constant pressure (30 bars) in two 4 metre test sections in KI0025F02 (L=73.3-77.3 m (Structure #20) at Q= 8.9 l/min and L=64.2-68.2 m (Structure #6 ?) at Q=3.7 l/min.

Preliminary results show that section KA2563A:R5 shows a marked increase in flow due to pumping, especially during pumping of section 73.3-77.3 m, cf. Figure 8-2a. In the case of pumping in 64.2-68.2 m an increase is observed as well, but it is not as big. In the case of section KI0023B:P6, an increase is observed due to pumping section 73.3-77.3 m, cf. Figure 8-2b, whereas no change is observed due to pumping of section 64.2-68.2 m

The results of the dilution tests in KI0025F:R4 are associated with a higher degree of uncertainty, and it is difficult to identify any significant effect of the two pumpings. This latter finding is puzzling since the section is located in a section (packing off Structure #20) which is characterised by a relatively high transmissivity ($T=1.8\cdot10^{-7}$ m^2/s) and the noted drawdown during the test in section 73.3-77.3 is high (870 kPa), suggesting a good hydraulic connection.

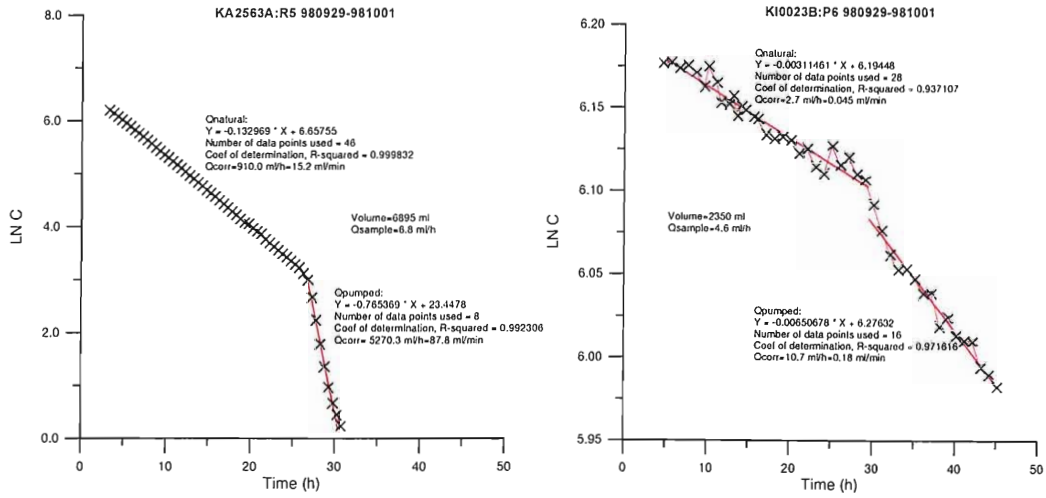

Figure 8-2 Tracer dilution curves before and during pumping in section 73.3-77.3m in KFI0025F02 for a) borehole section KA2563A:R5 and b) borehole section KI0023B:P6.

8.3.3 Tracer dilution tests in KI0025F02 during pumping in KI0023B

In this particular test, the test sequence is reversed to the one employed in the tests presented in Section 8.3.2. The objective was to further elucidate the mutual connectivity of Structures #9, #20 and #13. Three sections in KI0025F02 (KI0025F02:P3 (Structure #13), KI0025F02:P5 (Structure#20), KI0025F02:P8 (Structure #9) were used for tracer dilution tests under undisturbed and stressed conditions. The pumping was performed at constant pressure (23 bars) (Q=2.6 l/min) in KI0023B:P6 (Structure #9).

Preliminary results show very marked influences of the pumping, cf. Figure 8-3. Of particular interest is the result from section KI0025F02:P8, cf. Figure 8-3b. In this section a marked reduction of the flow rate is observed as a result of the pumping. This suggests that the natural flow rate, which is found to be comparatively high, has been reversed, or at least significantly decreased. Given the relative positioning of the borehole sections involved, partial support for the eastward flow direction in Structure #9 is obtained, cf. Section 7.2.2 and Figure 7-1.

Table 8-1 Compilation of combinations of sink and probable source sections in the TRUE Block Scale borehole array between which future tracer experiments potentially can be made.

Sink section	Probable source section	Less probable source section
KI0023B:P6 (#9)	KA2563A:R5 (#20) KI0025F02:P5 (#20) KI0025F02:P8 (#9) KI0025F02:P3 (#13)	KI0025F02:P6 (#6) KI0025F:R4 (#20)
KI0025F02:P5 (#20)	KA2563A:R5 (#20) KI0023B:P6 (#9) KI0025F:R4 (#20)	KI0025F02:P8 (#9) KI0025F02:P6 (#6) KI0025F02:P3 (#13)
KA2563A:R5 (#20)	KI0023B:P6 (#9) KI0025F02:P5 (#20) KI0025F02:P6 (#6)	KI0025F02:P8 (#9) KI0025F02:P3 (#13) KI0025F:R4 (#20)

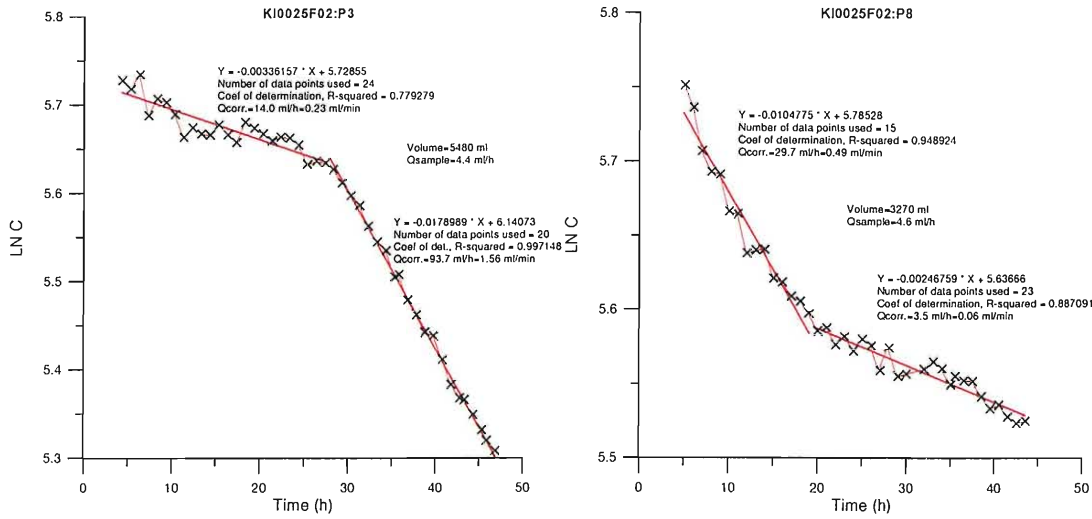

Figure 8-3 *Tracer dilution curve before and during pumping in borehole section KI0023B:P6 for a) borehole section KI0025F02:P3 and b) borehole section KI0025F02:P8.*

8.4 Proposed loci for future transport experiments

The combined results from the hydraulic interference tests, the transport experiments, and the dilution tests presented in the preceding sections show that a network of connected structures are available in the investigated TRUE Block Scale rock volume. This network features a mutually consistent hydraulic connectivity pattern as described in Section 7.1.1 of this report. Furthermore the results of one single successful tracer test performed to date show that a transport experiment can be performed in a fracture network over distances in excess of 16 metres.

The added information from the tracer dilution tests, although they do not provide a definite answer of likelihood of success, show that the prospects are good for experiments involving the structures mentioned above, cf. Sections 8.2 and 8.3.

Table 8-1 presents a list of candidate combinations of source and sink sections for future transport experiments.

It should be emphasised that tracer dilution tests have been conducted in only a selection of the sections listed in Table 8-1. There exists a need to investigate further the listed options through a series of pre-tests supported by modelling work, cf. Section 8.5.2 and Chapter 9.

Experiments conducted between the proposed sections cover a range of Cartesian distances between 16 to 50 m. It should be noted that tests with sorbing tracers over longer distances will be difficult to achieve over practical time frames.

8.5 Tracer test considerations

8.5.1 Types of tests

There are several types of tests/flow geometries which have been discussed and which may be used as part of planned future transport experiments. Among these are;

- *Radially converging flow geometry*. This type of test geometry is preferred and has proved to be an effective test during the performed TRUE-1 tracer tests [3]. The main disadvantage with this type of test is the relatively high dilution in the injection section. Two types of converging tests are possible;

- Point sink (one structure)
- Line sink (borehole sections including different structures, several borehole sections including the same structure, or alternatively a complete borehole length forming a distributed sink)

- *Unequal strength dipole flow geometry.* The advantage being less dilution and a reduction of the impact of local heterogeneity in the vicinity of the injection section.
- *Single hole tests.* This type of test employs location of the source and sink in the same borehole.

8.5.2 Pre-tests

A number of pre-tests are foreseen with the following objectives;

- Identification of optimal source and sink locations over shorter distances (10-25 m)
- Identification of source and sink pairs over longer distances (25-50 m)
- Assessment of tracer breakthrough and recovery

The number of tests has not been fixed at this stage, but a total of 2-5 tests appears reasonable to cover the range of possible source and sink locations. The tests will be of short duration and performed at maximum source strength and will also include initial assessment of change in section cross-flow using tracer dilution tests.

8.5.3 Proposed tracers

For the planned tracer tests within the TRUE Block Scale, 5-10 conservative tracers are needed. In the TRUE-1 tracer tests a number of conservative tracers have been employed, both non-radioactive and radioactive. The non-radioactive conservative tracers included; flourescent tracers such as Uranine, Rhodamine WT and Amino-G. Among possible radioactive tracers are tritiated water (HTO), Bromide ^{82}Br, Iodide ^{131}I. A restriction in use of radioactive tracers calls for additional non-radioactive tracers. A programme for testing of alternative additional conservative tracers is under way.

In the case of weakly sorbing tracers, the experience from the TRUE-1 tracer tests can be used [3]. Among tracers used are radioactive isotopes from the alkaline metal group (Na^+, Rb^+, Cs^+) and the alkaline earth metal group (Ca^{2+}, Sr^{2+} and Ba^{2+}). It is envisaged that a selection of these tracers will only be injected in a few flow paths.

9 Outlook on future work

This chapter outlines the avenue of approach for the concluding parts of the Detailed Characterisation Stage and the initial parts of the Tracer Test stage. However, prior to presenting the approach, the objectives of the project are revisited in light of the available data and inferences made in the previous chapters.

9.1 Revisit of project objectives

The experimental results, modelling results, and inferences made as presented in the preceding chapters show that;

1) we have identified an interconnected network of deterministic conductive structures that may be observed in a number of boreholes. The structures are relatively well known geometrically and structurally. Consistency in hydraulic connectivity is proven from observation of pressure responses during drilling and from hydraulic cross-hole interference tests,

2) we have identified relatively well-defined hydraulic structures which constitute boundaries to the outlined block,

3) we have a transmissivity range of the structures making up the identified network which is less than $7 \cdot 10^{-7}$ m^2/s,

4) we have a conceptual model for natural groundwater flow in the structures supported by geometrical, structural, hydraulic field data. Additional support is provided by performed numerical modelling and independent chemical data,

5) we have a number of candidate sections for establishing source and sink sections available in the borehole array,

6) we have demonstrated for one flow path that tracer tests can be successfully performed in the identified network of structures at a length scale in excess of 16 m over reasonable time frames.

The potential length scales in the identified network fit in to the originally set length scales stated in the test plan, cf. Chapter 2. The measured transmissivities indicated above are within a suitable and practical transmissivity range for tracer testing, in parity with the desired transmissivity range stated in the test plan, cf. Chapter 2.

With regards to radionuclide retention it was early on identified that the ultimate task in TRUE Block Scale is to apply the findings of the Detailed Scale TRUE experiment which is focused on a single fracture to the network of investigated in the TRUE Block Scale Experiment. An important question to be asked regards the relative impacts of the fracture network, fracture network intersections, and heterogeneity within individual structures on retention of radionuclides.

It was also early on identified that tests with moderately sorbing tracers could only be performed over short distances. In addition, any inference in the block scale has to rely on the results obtained from performed single fracture studies. It is projected in a fracture network, over distances in excess of 10 meters, only weakly sorbing tracers are possible to use for studies of retention.

Hence, to the overall objectives for the TRUE Block Scale Project given in Chapter 2, the following specific objectives for planned tracer tests are defined;

- Perform transport experiments in a network of structures made up of Structures #13, #9, #20, and possibly #6,
- Evaluate transport parameters from the performed tracer tests,
- Evaluate, to the extent possible, the effects on solute transport exerted by the heterogeneity within the fracture network (fracture intersections and heterogeneity within individual structures).

The following general work scope for future work has been identified;

- Assess existing sink and source sections for transport experiments, and combinations thereof, including need for complementary sections (including improved visualisation),
- Assess need to improve the structural model,
- Evaluate boundary conditions assigned to numerical models (including tunnel boundary condition),
- Improve and test numerical models using responses to interference data, primarily cross-hole interference test data and existing tracer dilution test results,
- Resolve identified needs by optimising the existing borehole array. This includes evaluation of the need for reaming KA2563A to facilitate more leadthroughs (more test sections). In addition drilling and characterisation of another exploration is retained as an option pending results of the planned pre-tests,
- Identify suitable pumping and injection sections in restored and/or new boreholes,
- Identify and test suitable conservative tracers,

- Define hypotheses to be tested by the planned tracer experiments,
- Design transport experiments over selected length scales (including run of tracer experiments using developed numerical models),
- Perform pre-tests with conservative tracers in the borehole array to find optimal combinations of source and sink sections (including tracer dilution tests and actual tracer experiments),
- Assess the need for an additional borehole to meet set up objectives,
- Perform transport experiments with conservative and weakly sorbing tracers in the selected array of borehole sections,
- Predict and evaluate the hydraulic experiments and transport experiments iteratively using available modelling tools.

10 References

[1] Bäckblom, G. and Olsson, O. 1994: Program for tracer retention understanding experiments. Swedish Nuclear Fuel and Waste Management Co. SKB Äspö Hard Rock Laboratory Progress Report PR 25-94-24.

[2] Winberg, A. 1997: Test plan for the TRUE Block Scale Experiment. Swedish Nuclear Fuel and Waste Management Co. Äspö Hard Rock Laboratory International Cooperation Report ICR 97-02.

[3] Winberg (ed.), et al. (in prep): Tracer Retention Understanding Experiments - First TRUE Stage Final Report (Tentative title). Swedish Nuclear Fuel and Waste Management Co. SKB Technical Report TR 99-XX.

[4] Svensson, U. 1997: A site scale analysis of groundwater flow and salinity distribution in the Äspö area. Swedish Nuclear Fuel and Waste Management Co. SKB Technical Report TR 97-17.

[5] Rhen, I. (ed.) et al. 1997: Results from pre-investigations and detailed site characterization. – Summary report. Swedish Nuclear Fuel and Waste Management Co. SKB Technical Report TR 97-03.

[6] Stanfors, R., Olsson, P., Stille, H. 1997: Results from pre-investigations and detailed site characterization – Comparison of predictions and observations – Geological and mechanical stability. Swedish Nuclear Fuel and Waste Management Co. SKB Technical Report TR 97-04.

Appendices

Appendix A

Configuration of test sections in instrumented boreholes as of May 1998.

N.B the indicated instrumentation given for boreholes KI0025F02 and KA3510A came into effect in mid October 1998.

Borehole section	Interval (meters)	September 1998 Model
KA2511A:S1	242.00-244.00	#18
KA2511A:S2	217.00-241.00	#10
KA2511A:S3	110.00-216.00	#17, #19, #20
KA2511A:S4	92.00-109.00	#6, #16
KA2511A:S5	52.00-54.00	#7
KA2563A:R1	262.00-363.00	#9, #10
KA2563A:R2	225.00-228.00	#19
KA2563A:R3	220.00-225.00	?
KA2563A:R4	191.00-219.00	#13, #18
KA2563A:R5	187.00-190.00	#20
KA2563A:R6	146.00-186.00	#6, #7
KI0025F:R1	169.00-194.00	Z
KI0025F:R2	164.00-168.00	#19
KI0025F:R3	89.00-163.00	?
KI0025F:R4	86.00-88.00	#20
KI0025F:R5	41.00-85.00	#6, #7
KI0025F:R6	3.50-40.00	#5
KI0023B:P1	113.70-200.70	#10
KI0023B:P2	111.25-112.70	#19
KI0023B:P3	87.20-110.25	?
KI0023B:P4	84.75-86.20	#13
KI0023B:P5	72.95-83.75	#18
KI0023B:P6	70.95-71.95	#9
KI0023B:P7	43.45-69.95	#6, #20
KI0023B:P8	41.45-42.45	#7
KI0023B:P9	4.60-42.45	#5
KI0025F02:P1	135.15-204.0	#10?
KI0025F02:P2	100.25-134.15	#19
KI0025F02:P3	93.40-99.25	#13
KI0025F02:P4	78.25-92.40	Tight section
KI0025F02:P5	73.30-77.25	#20
KI0025F02:P6	64.00-72.30	#6
KI0025F02:P7	56.10-63.00	?, low T feature
KI0025F02:P8	51.70-55.10	#9
KI0025F02:P9	38.50-50.70	#7
KI0025F02:P10	3.40-37.50	#5?
KA3510A:P1	122.02-150.10	?
KA3510A:P2	114.02-121.02	#15
KA3510A:P3	4.52-113.02	#2-6, #8, grouted
KA3573A:P1	18.00-40..10	#15
KA3573A:P2	4.50-17.00	#5
KA3600F:P1	22.00-50.10	#15?
KA3600F:P2	4.50-21.00	#5, #7?

Appendix B

Detailed description of intercepts of interpreted structures in the TRUE Block Scale borehole array used to construct the September 1998 Structural model [8].

	KA2563A				KA2511A				KA3510A				KI0025F				KI0023B				Width	Geology
Structures	Depth (m)	Width (cm)	Type	Strike/ dip	Depth (m)	Width (cm)	Type	Strike/ dip	Depth (m)	Width (cm)	Type	Strike/ dip	Depth (m)	Width (cm)	Type	Strike/ dip	Depth (m)	Width (cm)	Type	Strike/ dip	Average width	geological description
1	12.5	0.2	Frac	335/82																	1	Fgranite, fractured, faults, faults in the tunnel
2	68.5	220	Zone	135/87					11.1	15	Frac	309/75									110	Oxidized, fractured, crush
3	68.5	220	Zone	135/87					37.5	40	Zone	106/81									130	Oxidized, fractured, crush
4	94.4	6	Frac	296/74	23.1	10	Frac	300/80	12.9	8	Fault	115/89									10	Fgranite, greenstone, crush
5	103	2	Frac	114/89					47.7	10	Fault	138/75	4.9	10	Frac	307/57	7.2	5	Frac	112/87	10	Variable structure partly altered
6	153.4	140	Fault	111/73	100	0.2	Frac	340/71	56.7	0.5	Frac	131/87	76.6	80	Frac	107/65	44.2	10	Fault	103/87	50	oxidized network with faults
7	153.4	140	Fault	111/73	52.4	0.2	Frac	119/79					43.5	25	Frac	253/84	42.2	4	Frac	338/83	40	Oxidized, fractured, crush
8	242.4	8	Fault	026/84					16.1	100	Zone	232/89									50	Faultzone structure in TBM tunnel and KA3510, KA2563A
9	265.8	5	Fault	096/85													71.1	10	Frac	123/86	8	Oxidized, single open faults
10	351.3	25	Fault	124/80		0.5	Frac	127/85									171	30	Zone	298/83	20	Variable structure partly in greenstone
11					258	15	Fault	288/88													10	Visible as single fault in diorite
12																						Only observed by seismics, see Table XXX
13	207	20	Fault	321/86													85.6	15	Fault	318/89	17	Fault with altered and deformed diorite
15									118	60	Fault	269/88									60	Fgranite, crush (118-119 m in KA3510A)
16	56.3	120	Zone	011/40	105	100	Zone	233/18													110	Fgrained granite, oxidized
17	108.9	0.2 (140) 0.1	Frac	222/34	132	5 (230)	Frac	270/16													3 (190)	Fgrained granite, greenstone
18	194.3	(20)	Frac	012/18	243	10	Fault	155/9									75.5	80	Swarm	348/41	20	Fgrained granite
19	226.8	10	Fault	308/47	198	35	Frac	324/87					166.4	65	Zone	338/74	112	20	Fault	342/87	30	Faults in Finegrained granite, alteration
20	188.7	5 (60)	Fault	316/82	122	0.2 (100)	Frac/ Swarm	336/67					87.7	0.2	Frac	336/77	69.8	20	Fault	157/82	100	Open fault KA2563A, other intercepts faultgroups in altered diorite
Z													192.1	+550	Zone	243/77					+550	Minor branch of either EW-3 or NE-1

Appendix C

Results of chemical analyses made on groundwater samples collected in the instrumented borehole array September 1997-March 1998 (Data extracted from the SKB database SICADA)

IDCODE	DATE	IDCODE	SECUP (m)	SECLOW (m)	SAMPLE_NO	CLASS NO	NA (mg/l)	K (mg/l)	CA (mg/l)	MG (mg/l)	HCO3 (mg/l)	CL (mg/l)	SO4 (mg/l)	BR (mg/l)	FE (ICP) (mg/l)
KI0025F	970929 17:00:00	KI0025F	158.00	168.00	2435	4	2090	9.8	1630	45.7	11	6100	511	34.5	0.089
KI0025F	970929 17:00:00	KI0025F	86.00	88.00	2436	4	2200	9.0	1820	40.5	8	6670	463	45.0	0.032
KA2511A	970930 09:00:00	KA2511A	139.00	170.00	2438	4	1560	11.1	496	80.7	232	3380	335	13.4	0.276
KA2563A	970930 12:00:00	KA2563A	187.00	196.00	2437	4	2140	9.0	1670	44.6	10	6300	452	39.9	0.060
KI0023B	980305 09:40:00	KI0023B	111.25	112.70	2495	4	1780	8.9	1050	47.5	61	5060	345	27.5	0.115
KI0023B	980305 09:40:00	KI0023B	84.75	86.20	2496	4	2030	6.9	1450	41.5	15	6130	406	35.3	0.025
KI0023B	980305 09:40:00	KI0023B	70.95	71.95	2497	4	1920	7.8	1290	43.6	27	5590	367	29.8	0.048
KI0023B	980305 09:40:00	KI0023B	41.45	42.45	2498	4	1780	9.3	1030	60.2	97	5060	368	27.0	0.299
KI0025F	980305 09:41:00	KI0025F	164.00	168.00	2499	4	2100	9.0	1580	47.7	16	6190	424	34.0	0.110
KI0025F	980305 09:41:00	KI0025F	86.00	88.00	2500	4	2140	7.5	1540	46.4	17	6050	377	35.8	0.032
KA2511A	980305 16:30:00	KA2511A	92.00	109.00	2502	4	1600	10.9	452	97.9	217	3350	315	13.6	0.437
KA2511A	980305 16:30:00	KA2511A	52.00	54.00	2503	4	1650	7.6	748	88.1	170	4080	263	15.5	0.493
KA2563A	980305 16:30:00	KA2563A	187.00	190.00	2504	4	1960	9.0	1170	61.8	80	5160	335	21.8	0.138
KA3573A	980309 10:03:00	KA3573A	18.00	40.70	2511	4	1650	9.9	539	91.7	209	3530	311	16.1	0.347
KA3573A	980309 10:03:00	KA3573A	4.50	17.00	2512	4	1730	9.7	603	91.7	213	3780	295	17.1	0.312
KA3600F	980309 10:05:00	KA3600F	22.00	50.10	2513	4	1880	13.5	714	105.0	225	4260	277	21.4	0.373
KA3600F	980309 10:05:00	KA3600F	4.50	21.00	2514	4	1750	9.4	656	91.3	194	3730	298	18.0	0.289

IDCODE	DATE	IDCODE	SECUP	SECLOW	SAMPLE_NO	CLASS NO	FE (Spectr)	MN	LI	SR	PH	COND	DOC	D	O18

			(m)	(m)			(mg/l)	(mg/l)	(mg/l)	(mg/l)		(mS/m)	(mg/l)	dev SMOW	dev SMOW
KI0025F	970929 17:00:00	KI0025F	158.00	168.00	2435	4		0.26	1.09	28.7	7.7	1620	1.2	-74.50	-9.3
KI0025F	970929 17:00:00	KI0025F	86.00	88.00	2436	4		0.23	1.32	28.7	8.0	1740	1.0	-83.50	-10.5
KA2511A	970930 09:00:00	KA2511A	139.00	170.00	2438	4	0.335	0.52	0.24	8.39	7.4	1000	4.2	-64.10	-7.5
KA2563A	970930 12:00:00	KA2563A	187.00	196.00	2437	4	0.070	0.30	1.19	29.1	7.4	1710	1.1	-78.00	-9.9
KI0023B	980305 09:40:00	KI0023B	111.25	112.70	2495	4	0.132	0.38	0.811	18.8	7.3	1440	2.6	-69.00	-8.7
KI0023B	980305 09:40:00	KI0023B	84.75	86.20	2496	4	0.040	0.30	1.13	24.1	7.6	1720	1.6	-87.30	-11.3
KI0023B	980305 09:40:00	KI0023B	70.95	71.95	2497	4	0.067	0.33	0.942	20.6	7.4	1570	2.9	-72.20	-9.2
KI0023B	980305 09:40:00	KI0023B	41.45	42.45	2498	4	0.306	0.45	0.716	17.0	7.4	1420	3.8	-70.00	-8.8
KI0025F	980305 09:41:00	KI0025F	164.00	168.00	2499	4		0.28	1.04	26.2	7.7	1740	2.0	-77.10	-9.6
KI0025F	980305 09:41:00	KI0025F	86.00	88.00	2500	4		0.24	0.99	24.7	7.7	1720	2.4	-77.50	-9.8
KA2511A	980305 16:30:00	KA2511A	92.00	109.00	2502	4	0.471	0.60	0.20	7.29	7.4	1160	6.5	-60.70	-7.3
KA2511A	980305 16:30:00	KA2511A	52.00	54.00	2503	4	0.525	0.60	0.38	12.2	7.3	1140	4.7	-68.00	-8.3
KA2563A	980305 16:30:00	KA2563A	187.00	190.00	2504	4	0.170	0.38	0.76	17.5	7.3	1440	3.7	-71.00	-8.8
KA3573A	980309 10:03:00	KA3573A	18.00	40.70	2511	4	0.382	0.53	0.25	8.34	7.4	882	5.5	-61.00	-7.4
KA3573A	980309 10:03:00	KA3573A	4.50	17.00	2512	4	0.351	0.54	0.28	9.23			6.6	-61.40	-7.5
KA3600F	980309 10:05:00	KA3600F	22.00	50.10	2513	4	0.386	0.67	0.38	11.4	7.2	1330	5.5	-62.10	-7.7
KA3600F	980309 10:05:00	KA3600F	4.50	21.00	2514	4	0.338	0.51	0.30	9.31	7.3	1120	14.6	-63.00	-7.6